isothermal amplification (LAMP), that amplifies DNA with high specificity, efficacy, and rapidity under isothermal conditions. The LAMP reaction requires a *Bst* DNA polymerase with strand displacement activity and a set of four specially designed primers that recognize six distinct sequences on the target DNA, the specificity of which should be extremely high. The amplification products are stem-loop DNA structures with several inverted repeats of the target. The advantage of the LAMP method is that the reaction is performed under isothermal conditions of between 60 and 65 °C. As a result, it requires only simple and cost-effective reaction equipment. The LAMP method has emerged as a powerful tool to facilitate genetic testing for various infectious diseases (Enosawa *et al.*, 2003; Iwamoto *et al.*, 2003; Kuboki *et al.*, 2003; Ihira *et al.*, 2004; Parida *et al.*, 2004; Thai *et al.*, 2004).

The purpose of our work is to identify a species-specific region of *Mycobacterium* sp., and to develop a LAMP assay that can differentiate clinically relevant species.

Materials and methods

Bacterial strains and preparation of genomic DNA

The bacteria used in this study comprised 27 strains and 49 clinical isolates as shown in Table 1. All strains except for *Mycobacterium leprae* were cultured on 1% Ogawa medium (Nissui, Tokyo, Japan) at 37 °C. *Mycobacterium leprae* was prepared from infected nude mouse food pad (Shepard, 1960). Genomic DNA was extracted from mycobacterial strains as follows. Mycobacterial cells were resuspended in 1.8 mL of sterile phosphate-buffered saline (PBS) containing 0.1 mm diameter zirconia/silica beads (BioSpec Products Inc., Bartlesville, OK). The mixture was beaded for 20 s with a Beads Homogenizer Model BC-20 (Central Scientific Commerce, Tokyo, Japan), transferred to a 1.5 mL microcentrifuge tube, and the genomic DNA was purified with proteinase K treatment and phenol/chloroform extraction followed by ethanol precipitation, then suspended in 100 μL distilled water.

Table 1. *Mycobacterium* species and strains used in this study and results of the loop-mediated isothermal amplification assay

			Primer set	
Species	Strains	Accession number	Kan32	Gas583
Mycobacterium abscessus	JATA 63-01 (ATCC 19977)	AB087684	–	–
Mycobacterium africanum	KK 13-02 (ATCC 25420)	AB087685	–	–
Mycobacterium avium	JATA 51-01 (ATCC 25291)	AB087686	–	–
	Clinical isolate 22 strains			
Mycobacterium bovis	JATA 12-01 (ATCC 19210)	AB087687	–	–
Mycobacterium chelonae	JATA 62-01 (ATCC 35752)	AB087688	–	–
Mycobacterium fortuitum	JATA 61-01 (ATCC 6841)	AB087689	–	–
Mycobacterium gastri	KK 44-02 (ATCC 15754)	AB087690	–	+
Mycobacterium gordonae	JATA 33-01 (ATCC 14470)	AB087691	–	–
Mycobacterium intracellulare	JATA 52-01 (ATCC 13950)	AB087692	–	–
	Clinical isolate 17 strains			
Mycobacterium kansasii	KK 21-01 (ATCC 12478)	AB087693	+	–
	Clinical isolate 10 strains		+	–
Mycobacterium leprae	Thai-53	AB087694	–	–
Mycobacterium malmoense	JATA 47-01 (ATCC 29571)	AB087695	–	–
Mycobacterium marinum	JATA 22-01 (ATCC 927)	AB087696	–	–
Mycobacterium microti	KK 14-01 (ATCC 19422)	AB087697	–	–
Mycobacterium nonchromogenicum	JATA 45-01 (ATCC 19530)	AB087698	–	–
Mycobacterium parafortuitum	ATCC 25807	AB087699	–	–
Mycobacterium phlei	ATCC 19249	AB087700	–	–
Mycobacterium scrofulaceum	JATA 31-01 (ATCC 19981)	AB087701	–	–
Mycobacterium simiae	KK 23-08 (ATCC 25275)	AB087702	–	–
Mycobacterium smegmatis	JATA 64-01	AB087703	–	–
Mycobacterium szulgai	JATA 32-01	AB087704	–	–
Mycobacterium terrae	KK 46-01 (ATCC 15755)	AB087705	–	–
Mycobacterium triviale	KK 50-02 (ATCC 23292)	AB087706	–	–
Mycobacterium tuberculosis	JATA 11-01 (H37Rv)	AB087707	–	–
Mycobacterium ulcerans	KK 43-01	AB087708	–	–
Mycobacterium vaccae	KK 66-01	AB087709	–	–
Mycobacterium xenopi	KK 42-01 (ATCC 19250)	AB087710	–	–

All strains were kindly donated by Dr Kashiwabara, NIID.

Clinical isolates were identified by Amplicore *Mycobacterium* kit (Roche Pharma, Basel, Switzerland) or conventional biochemical test (Jamal *et al.*, 2000).

Amplification of the region within *dnaA* gene

Highly polymorphic regions flanked by conserved regions were identified by aligning the *Mycobacterium* spp. *dnaA* sequences, which were available in GenBank at the time this study was initiated. These regions were used to design a pair of degenerate primers, U1F 5′-GTS CAR AAC GAR ATC GAR CG-3′ and U1R 5′-CCB GAY TCR CCC CAG ATG AA-3′. A schematic representation of the primer design is shown in Fig. 1a. PCR was performed in a TAKARA Thermal Cycler MP (TAKARA Biomedical, Otsu, Japan) with a reaction mixture consisting of 1 μL of genomic DNA, each deoxynucleoside triphosphate at a concentration of 200 μM, each primer at a concentration of 0.4 μM, 1 × PCR buffer with 1.5 mM $MgCl_2$ (TAKARA Biomedical), and 1.25 U of ExTaq (TAKARA Biomedical), with 10 μL PCRX Enhancer System solution (Gibco BRL, Rockville, MD) in a total volume of 50 μL. The PCR thermocycles were 3 min at 94 °C, followed by 30 cycles of 94 °C for 10 s, 50 °C for 20 s, and 72 °C for 45 s, with a final extension step at 72 °C for 7 min. PCR products were visualized by UV illumination of an ethidium bromide-stained 1.5% agarose gel and cut out to purify with EASYTRAP Ver.2 (TAKARA Biomedical) according to the manufacturer's instruction.

DNA sequencing and sequencing analysis

The ABI Prism BigDye Terminator v3.1 Cycle Sequencing Kit (PE Biosystems, Foster City, CA) was used for the sequencing of the PCR products. The same primers for amplification were used for sequencing. The sequencing reaction was performed in accordance with the instruction of the manufacturer. Sequencing products were purified with a Centrisep column (Princeton Separations, Adelphia, NJ).

The sequencing output was analyzed by using the DNA Sequence Analyzer computer software (PE Biosystems). The partial *dnaA* sequences were aligned using the Clustal W algorithm (Thompson *et al.*, 1994) of the software DNASpace ver. 3.5 (Hitachi Software Engineering, Yokohama, Japan), and the alignment was manually corrected. A phylogenetic tree was generated by DNASpace ver. 3.5 (Hitachi Software Engineering) with a total of 1000 bootstraps. Pairwise similarity of the partial *dnaA* sequences was determined by using DNASIS package (Hitachi Software Engineering).

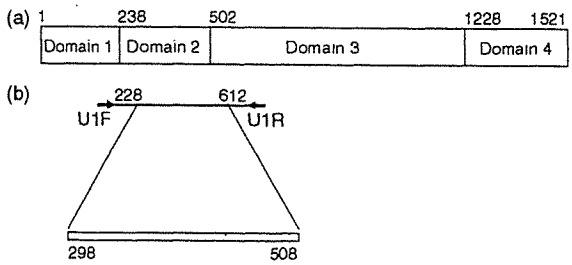

Fig. 1. Schematic representation of the DnaA protein and primer design for the amplification of the partial mycobacterial *dnaA* gene. Number indicates the nucleotide position of *Mycobacterium tuberculosis*, GenBank accession number AL021427. (a) The DnaA protein from *M. tuberculosis* contains four domains. Domain 1 is involved in interaction with DnaB. Domain 2 constitutes a flexible loop. DNA unwinding required Domain 3. Domain 4 is sufficient for specific binding to DNA. Primers U1F and U1R were used to generate about 400 bp fragment from *dnaA* of 27 mycobacterial spp. (b) Analysis and comparison region used in this study are indicated by a bar (298–508 bp).

Species-specific LAMP assay for *Mycobacterium kansasii* and *Mycobacterium gastri*

A set of four primers comprising two inner primers and two outer primers that recognized six distinct regions on the target sequence were designed with PrimerExplorer Ver.3 (Fujitu, Tokyo, Japan). The detailed sequences of the primers are shown in Fig. 3. The two inner primers are called the forward inner primer (FIP) and the backward inner primer (BIP), and each contains two distinct sequences corresponding to the sense and antisense sequences of the target DNA, one for priming in the first stage and the other for self-priming in late stages. FIP contains the sequence complementary F1 (F1c) and F2. BIP contains the complementary B1 (B1c) and B2. The two outer primers consist of F3 and B3.

The LAMP reaction was carried out in 25 μL of reaction mixture by using the Loopamp DNA amplification kit (Eiken Chemical Co. Ltd., Tochigi, Japan) containing 2.4 μM (each) FIP and BIP, 0.2 μM (each) of the outer primers, F3 and B3, 20 mM Tris-HCl (pH 8.8), 10 mM KCl, 8 mM $MgSO_4$, 10 mM $(NH_4)_2SO_4$, 0.1% Tween 20, 0.8 M betaine, 1.4 mM (each) of dNTP, 8 U of *Bst* DNA polymerase (New England BioLabs, Beverly, MA), and the template DNA. Amplification was undertaken in 0.5 μL microtubes in a heatblock under isothermal conditions of 63 °C for 60 min, followed by 80 °C for 2 min to terminate the reaction. Positive and negative controls were included in each run, and precautions to prevent cross-contamination were observed. Two microliter aliquots of LAMP products were subjected to electrophoresis on a 4% agarose gel in Tris-borate-EDTA buffer followed by staining with ethidium bromide and were visualized on a UV transilluminator at 302 nm. The specificity of the LAMP-amplified products were further validated by restriction enzyme digestion with *Nae*I and *Hae*II for *M. kansasii* and *M. gastri*, respectively. The diluted genomic DNA was used for determining the sensitivity of the species-specific LAMP assay.

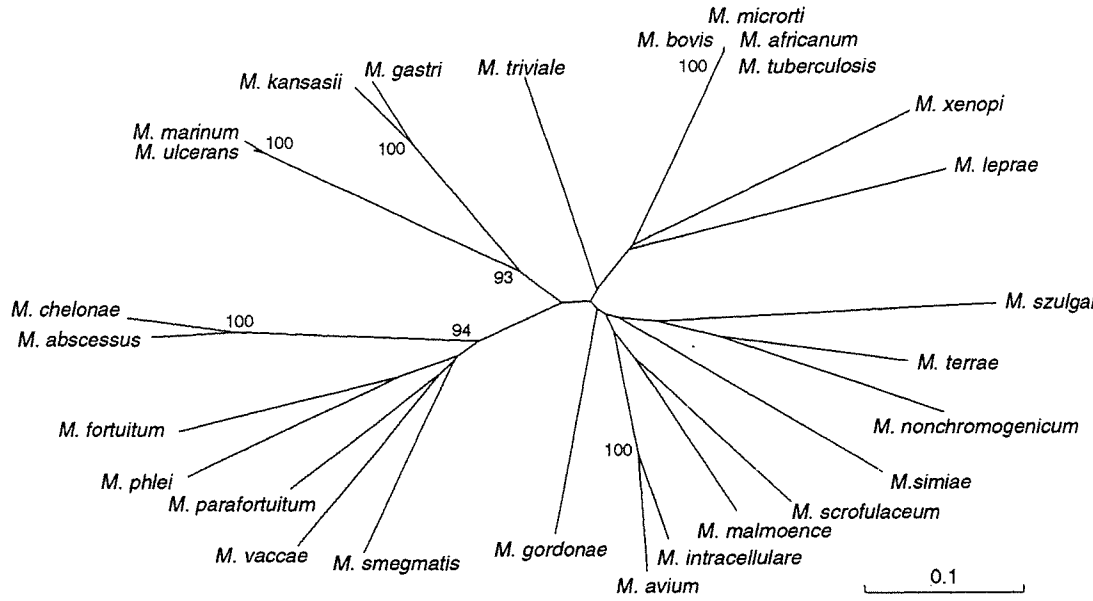

Fig. 2. Phylogenetic relationship of 27 *Mycobacterium* species. Unrooted tree based on the *dnaA* sequences. The tree was generated from DNASpace (Hitachi Software Engineering) with the Clustal W algorithm. The numbers on the dendrogram indicate the percentages of occurrence in 1000 bootstrapped trees; only values of > 90% are shown.

Results

Comparison of partial *dnaA* sequence to identify the *Mycobacterium* species

For the species identification of mycobacterial species, we analyzed some possible variable regions of mycobacterial sequences deposited in the GenBank, and found the 5′ part of the *dnaA* gene as a candidate target for PCR amplification. The PCR products with U1F and U1R, from 27 mycobacterial species, showed the ragged pattern around 400 bp in size (data not shown). Therefore, we determined nucleotide sequences, corresponding to position 228–612 bp of *Mycobacterium tuberculosis*, of all 27 species (Fig. 1a). The alignment of the sequence shows that the region (298–508 bp) in the amplified products had the highest species-specific variability (Fig. 1b). The size of the variable fragment in *dnaA* ranged from 154 bp in *M. triviale* to 232 bp in *M. kansasii*. The variable region exhibits a reasonable number of nucleotide substitution and insertion or deletion sites, which is important for the development of a differential diagnostic tool. The lowest interspecies similarity was 28.2% in *M. leprae* versus *M. vaccae*. The similarity between *M. avium* and *M. intracellulare* was 78.3% and that between *M. marinum* and *M. ulcerans* was 97.7%. Pathogenic *M. kansasii* were easily differentiated from nonpathogenic *M. gastri* (83.6%). The sequences of *M. tuberculosis*, *M. microti*, *M. africanum*, and *M. bovis* were found to be identical, except for one nucleotide substitution that occurred in *M. bovis*. When clinical isolates from clinically relevant mycobacterial strains were analyzed, the following minor variation was found among each species: 97.7–100% (*M. avium*) and 96.0–100% (*M. intracellulare*). We did not find any intraspecies variation in 10 clinical isolates and the standard strain of *M. kansasii*. Because other reports using different systems revealed the existence of more than one sequevar (Yang *et al.*, 1993; Alcaide *et al.*, 1997), we may need to examine a bigger number of clinical isolates.

The unrooted phylogenetic tree showed that the 27 mycobacterial species were resolved by the variable region in the *dnaA* sequence (Fig. 2). All rapidly growing species, *M. abscessus*, *M. chelonae*, *M. fortuitum*, *M. parafortuitum*, *M. phlei*, *M. vaccae*, and *M. smegmatis*, made a cluster that was clearly separated from those of the other species so far examined. On the other hand, *M. kansasii*, *M. gastri*, *M. avium*, and *M. intracellulare* are clinically relevant species; however, the branch of the former two species was obviously segregated from one of the later two species, which was supported by high bootstrap values. The results indicated that the partial *dnaA* sequence could be useful for the differentiation of NTM (Fig. 2).

Identification of mycobacteria by *dnaA* sequence-targeted species-specific LAMP assay

Several sets of primers designed from the *dnaA* sequence were evaluated for their specificity and sensitivity by the LAMP method. One set of primers named Kan-32 for *M. kansasii* and Gas-583 for *M. gastri* was selected (Fig. 3), and

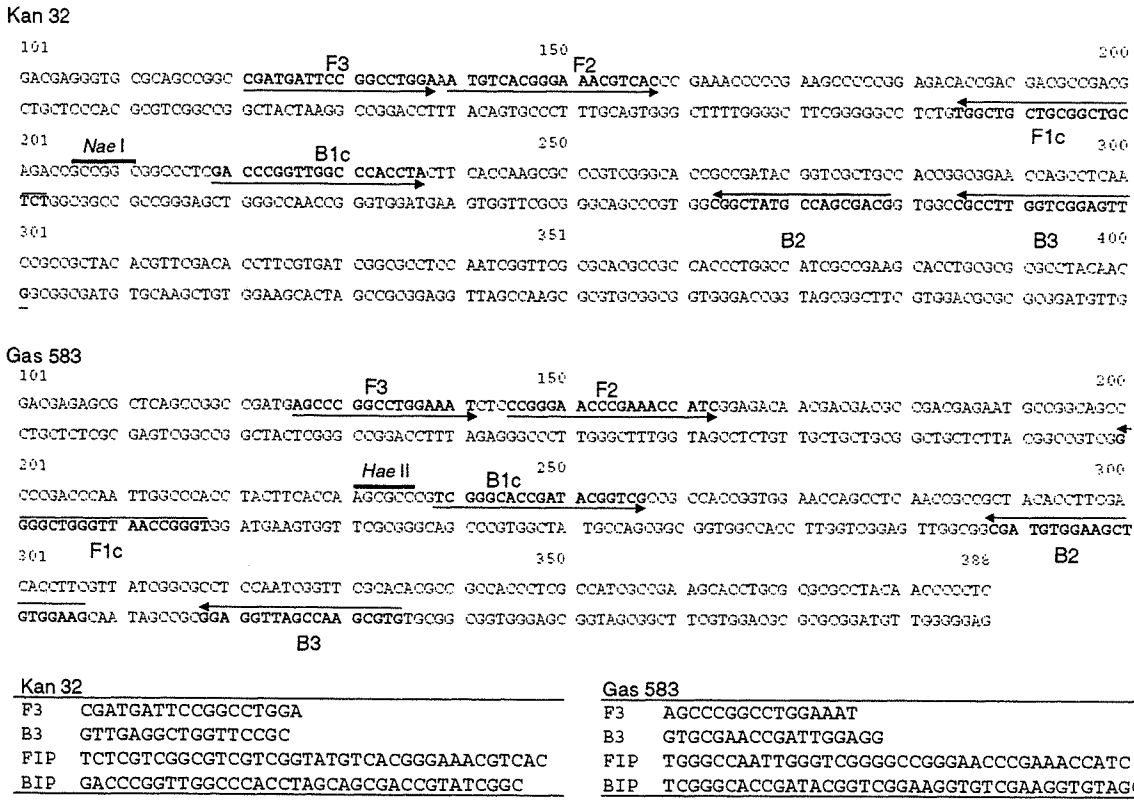

(b)

Kan 32	
F3	CGATGATTCCGGCCTGGA
B3	GTTGAGGCTGGTTCCGC
FIP	TCTCGTCGGCGTCGTCGGTATGTCACGGGAAACGTCAC
BIP	GACCCGGTTGGCCCACCTAGCAGCGACCGTATCGGC

Gas 583	
F3	AGCCCGGCCTGGAAAT
B3	GTGCGAACCGATTGGAGG
FIP	TGGGCCAATTGGGTCGGGGCCGGGAACCCGAAACCATC
BIP	TCGGGCACCGATACGGTCGGAAGGTGTCGAAGGTGTAGC

Fig. 3. Location of oligonucleotide primer sets Kan 32 and Gas 583, used for the loop-mediated isothermal amplification method. For *Mycobacterium kansasii* partial *dnaA* gene (GenBank accession number AB087693) and for *Mycobacterium gastri* partial *dnaA* gene (GenBank accession number AB087690). A right arrow indicates the sense sequence which is used as the primer. A left arrow indicates that a complementary sequence is used as the primer. The unique restriction enzyme recognition sites in the amplified product are shown with a bold bar. (b) List of each primer sequence.

by using these primer sets, a successful LAMP product appeared as a ladder of multiple bands (Fig. 3a).

The species specificity and intraspecies stability of each primer set were examined with purified DNA from 27 mycobacterial species and 10 clinical isolates of *M. kansasii*. We subjected each sample to amplification using Kan-32 or Gas-583 primer set. The results obtained by electrophoretic examination are summarized in Table 1. Although 200 pg of nontargeted species DNA were not amplified, significant amplification of targeted respective isolates was observed after a 60 min incubation at 63 °C. To confirm that the amplification products had corresponding DNA structures, the amplified products were digested with restriction enzymes and the size of the fragments was analyzed by electrophoresis. *Nae*I cuts between F1 and B1c for the *M. kansasii* amplicon; *Hae*II was used for the *M. gastri* amplicons. The sizes of the fragments generated after digestion were in good agreement with sizes predicted theoretically from the expected DNA structure: 100 and 93 bp by *Nae*I digestion, and 123 and 98 bp by *Hae*II digestion (Fig. 4a). Thus, we concluded that each primer set was species specific.

We next assessed the sensitivity of the assay. Serially diluted *M. kansasii* or *M. gastri* genomic DNA was used. The results of a typical experiment are shown in Fig. 4b. Amplified DNA was readily visible when 500 copies of genomic DNA were present in a 60 min incubation assay. The detection limit did not change with a longer incubation period (data not shown).

Discussion and conclusions

For the identification of species, a target gene must be conserved among strains and species. As the DnaA protein is generally conserved among microbial organisms (Mizrahi *et al.*, 2000), this coding region could be used for the target analysis. Four functional domains of the DnaA protein have been defined (Messer *et al.*, 1998). Domain 1 is involved in oligomerization and interaction with DnaB, Domain 2 constitutes a flexible loop, Domain 3 has ATPase function, and Domain 4 is sufficient for specific binding to DNA. The variable region that we identified in the *dnaA* sequence was equivalent to the Domain 2 coding nucleotide sequence

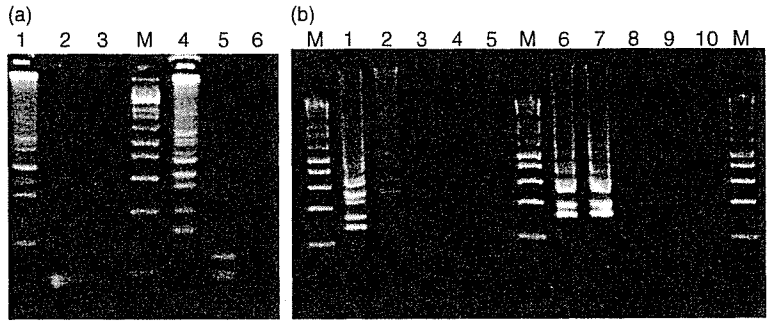

Fig. 4. (a) Four percent agarose gel electrophoresis and restriction enzyme analysis of loop-mediated isothermal amplification (LAMP) products of partial *dnaA* gene of *Mycobacterium kansasii* and *Mycobacterium gastri*. Lanes: M, 100 bp DNA ladder; lanes 1–3, LAMP carried out with *M. kansasii* primer, Kan 32, in the presence of genomic DNA from *M. kansasii* (lanes 1 and 2) and *M. gastri* (lane 3); lane 2, LAMP product from lane 1 after digestion with *Nae* I; lanes 4–6, LAMP carried out with *M. gastri* primer, Gas 583, in the presence of genomic DNA from *M. gastri* (lanes 4 and 5) and *M. kansasii* (lane 6). lane 5, LAMP product from lane 4 after digestion with *Hae* II. (b) Serial dilution of purified *M. kansasii* or *M. gastri* genomic DNA was amplified to determine the sensitivities by LAMP. Lanes: M, 100 bp DNA ladder; lanes 1–5 LAMP carried out with Kan 32 primer set in the presence of genomic DNA of *M. kansasii*, lane 1, 1000 copies; lane 2, 500 copies; lane 3, 100 copies; lane 4, 10 copy; lane 5, distilled water. lanes 6–10 LAMP carried out with gas 583 primer set in the presence of genomic DNA of *M. gastri*, lane 6, 1000 copies; lane 7, 300 copies; lane 8, 100 copies; lanes 9, 10 copy; lane 10, distilled water.

(Fig. 1). This domain is the least conserved region in the *dna A* gene with respect to sequence and length among *M. smegmatis*, *M. tuberculosis*, and *M. leprae* (Fsihi *et al.*, 1996). However, comparative studies of this region using 27 mycobacteria have not been reported and, as far as we know, this is the first report indicating the usefulness of the *dnaA* Domain 2 sequence as a differential diagnostic tool.

An accurate and rapid bacterial identification greatly contributes to this field of medication. Several methods based on molecular biological techniques have been reported. The sequences that have been reported include *hsp65*, 16S rRNA gene, and ITS (Plikaytis *et al.*, 1992; De Smet *et al.*, 1995; Springer *et al.*, 1996; Messer & Weigel, 1997; Roth *et al.*, 1998; Brunello *et al.*, 2001). Each gene has several advantages and disadvantages. An excessive degree of variability is found in the *hsp65* gene (Telenti *et al.*, 1993), which may hinder the development of reliable probes. While 16s rRNA gene sequence is identical in *M. kansasii* and *M. gastri* and shows narrow divergenicity within species (Taylor *et al.*, 1997), ITS sequence can be used to distinguish between *M. kansasii* and *M. gastri* (Roth *et al.*, 1998). While *M. kansasii* is a representative pathogenic mycobacteria, *M. gastri* does not induce an apparent disease. The discrimination between these mycobacteria provides useful information to select the appropriate therapy. The percent similarity of ITS between two species was 93% (Roth *et al.*, 1998), and that of the *dnaA* variable region was found to be 83.6%. These observations may indicate the usefulness of the *dnaA* gene for discrimination of these species, at least in complement with ITS.

The recent trend in genetic testing is to make systems fully automatic with high-throughput analysis. Although this may be an ideal approach, it requires expensive equipment as well as a well-trained person in diagnostic laboratories. The LAMP method could be conducted under isothermal conditions ranging from 60 to 65 °C by a single enzyme. The only equipment needed for LAMP reaction is a regular laboratory water bath or a heat block that furnishes a constant temperature around 63 °C. LAMP does not require a thermal cycling step, and an isothermal reaction for a short time (60 min) is enough to amplify the target DNA to a detectable level. As PCR and other molecular biological techniques are conducted in well-equipped laboratories, these methodologies are often impracticable under a field diagnosis.

In this paper, we demonstrated that the *dnaA* region could be an effective new nucleotide region for the diagnosis of NTM infection and that the LAMP method could be applied for a *dnaA* gene-based differential diagnostic tool.

Acknowledgements

We are grateful to Dr Y. Kashiwabara for the mycobacterial strains. This work was supported in part by a Health Science Research Grants-Research on Emerging and Re-emerging Infectious Diseases, Ministry of Health, Labour and Welfare, Japan.

References

Alcaide F, Richter I, Bernasconi C, Springer B, Hagenau C, Schulze-Robbecke R, Tortoli E, Martin R, Bottger EC & Telenti A (1997) Heterogeneity and clonality among isolates of *Mycobacterium kansasii*: implications for epidemiological and pathogenicity studies. *J Clin Microbiol* **35**: 1959–1964.

American Thoracic Society (1997) Diagnosis and treatment of diseases caused by nontuberculous mycobacteria. *Am J Respir Crit Care Med* **156**: S1–S25.

De Beenhouwer H, Liang Z, De Rijk P, Van Eekeren C & Portaels F (1995) Detection and identification of mycobacteria by DNA amplification and oligonucleotide-specific capture plate hybridization. *J Clin Microbiol* **33**: 2994–2998.

Blackwood KS, He C, Gunton J, Turenne CY, Wolfe J & Kabani AM (2000) Evaluation of *recA* sequences for identification of *Mycobacterium* species. *J Clin Microbiol* **38**: 2846–2852.

Brunello F, Ligozzi M, Cristelli E, Bnora S, Tortoli E & Fontana R (2001) Identification of 54 mycobacterial species by PCR-restriction fragment length polymorphism analysis of the *hsp65* gene. *J Clin Microbiol* **39**: 2799–2806.

Cernoch PL, Enns RK, Saubolle MA & Wallace RA Jr (1994) Laboratory diagnosis of the Mycobacterioses. Cumitech 16A (Weissfield AS, Coordinating ed.), American Society for Microbiology, Washington, DC.

Cloud JL, Neal H, Rosenberry R, Turenne CY, Jama M, Hillyard DR & Carroll1 KC (2002) Identification of *Mycobacterium* spp. by using a commercial 16S ribosomal DNA sequencing kit and additional sequencing libraries. *J Clin Microbiol* **40**: 400–406.

De Smet KA, Brown IN, Yates M & Ivanyi J (1995) Ribosomal internal transcribed spacer sequences are identical among *Mycobacterium avium–intracellulare* complex isolates from AIDS patients, but vary among isolates from elderly pulmonary disease patients. *Microbiology* **141**: 2739–2747.

Enosawa M, Kageyama S, Sawai K, Watanabe K, Notomi T, Onoe S, Mori Y & Yokomizo Y (2003) Use of loop-mediated isothermal amplification of the IS900 sequence for rapid detection of cultured *Mycobacterium avium* subsp. *paratuberculosis*. *J Clin Microbiol* **41**: 4359–4365.

Fsihi H, De Rossi E, Salazar L, Cantoni R, Labo M, Riccardi G, Takiff HE, Eiglmeier K, Bergh S & Cole ST (1996) Gene arrangement and organization in approximately 76 kb fragment encompassing the *oriC* region of the chromosome of *Mycobacterium leprae*. *Microbiology* **142**: 3147–3161.

Horsburg CR Jr (1991) *Mycobacterium avium* complex infection in the acquired immunodeficiency syndrome. *N Engl J Med* **324**: 1332–1338.

Ihira M, Yoshikawa T, Enomoto Y, *et al.* (2004) Rapid diagnosis of human herpesvirus 6 infection by a novel DNA amplification method, loop-mediated isothermal amplification. *J Clin Microbiol* **42**: 140–145.

Iwamoto T, Sonobe T & Hayashi K (2003) Loop-mediated isothermal amplification for direct detection of *Mycobacterium tuberculosis* complex, *M. avium*, and *M. intracellulare* in sputum samples. *J Clin Microbiol* **41**: 2616–2622.

Jamal MA, Maeda S, Nakata N, Kai M, Fukuchi K & Kashiwabara Y (2000) Molecular basis of clarithromycin-resistance in *Mycobacterium avium intracellulare* complex. *Tuberc Lung Dis* **80**: 1–4.

Kasai H, Ezaki T & Harayama S (2000) Differentiation of phylogenetically related slowly growing mycobacteria by their *gyrB* sequences. *J Clin Microbiol* **38**: 301–308.

Kim BJ, Lee SH, Lyu MA, Kim SJ, Bai GH, Chae GT, Kim EC, Cha CY & Kook YH (1999) Identification of mycobacterial species by comparative sequence analysis of the RNA polymerase gene (*rpoB*). *J Clin Microbiol* **37**: 1714–1720.

Kirschner P, Springer B, Vogel U, Meier A, Wrede A, Kiekenbeck M, Bange FC & Bottger EC (1993) Genotypic identification of mycobacteria by nucleic acid sequence determination: report of a 2-year experience in a clinical laboratory. *J Clin Microbiol* **31**: 2882–2889.

Kuboki N, Inoue N, Sakurai T, Di Cello F, Grab DJ, Suzuki H, Sugimoto C & Igarashi I (2003) Loop-mediated isothermal amplification for detection of African trypanosomes. *J Clin Microbiol* **41**: 5517–5524.

Messer W, Blaesing F, Majka J, *et al.* (1998) Functional domains of Dna A proteins. *Biochimie* **81**: 819–825.

Messer W & Weigel C (1997) Dna A initiator – also a transcription factor. *Mol Microbiol* **24**: 1–6.

Metchock BG, Nolte FS & Wallace RJ Jr (1999) *Mycobacterium. Manual of Clinical Microbiology*, 7th edn (Murray PR, Baron EJ, Pfaller MA, Tenover FC & Yolken RH, eds), pp. 399–437. American Society for Microbiology, Washington, DC.

Mizrahi VS, Dawes S & Rubin H (2000) DNA replication. *Molecular Genetics of Mycobacteria* (Hatful GF & Jacobs WR Jr, eds), pp. 159–172. American Society for Microbiology, Washington, DC.

Montessori V, Phillips P, Montaner J, Haley L, Craib K, Besşuille E & Black W (1996) Species distribution in human immunodeficiency virus-related mycobacterial infections: implications for selection of initial treatment. *Clin Infect Dis* **22**: 989–992.

Notomi T, Okayama H, Masubuchi H, Yonekawa T, Watanabe K, Amino N & Hase T (2000) Loop-mediated isothermal amplification of DNA. *Nucleic Acids Res* **28**: E63.

Parida M, Posadas G, Inoue S, Hasebe F & Morita K (2004) Real-time reverse transcription loop-mediated isothermal amplification for rapid detection of West Nile virus. *J Clin Microbiol* **42**: 257–263.

Park H, Jang H, Kim C, Chung B, Chang CL, Park SK & Song S (2000) Detection and identification of mycobacteria by amplification of the internal transcribed spacer regions with genus- and species-specific PCR primers. *J Clin Microbiol* **38**: 4080–4085.

Plikaytis BB, Plikaytis BD, Yakrus MA, Butler WR, Woodley CL, Silcox VA & Shinnick TM (1992) Differentiation of slowly growing *Mycobacterium* species, including *Mycobacterium tuberculosis*, by gene amplification and restriction fragment length polymorphism analysis. *J Clin Microbiol* **30**: 1815–1822.

Primm TP, Lucero CA & Falkinham JO III (2004) Health impacts of environmental mycobacteria. *Clin Microbiol Rev* **17**: 98–106.

Roth A, Fischer M, Hamid ME, Michalke S, Ludwig W & Mauch H (1998) Differentiation of phylogenetically related slowly growing mycobacteria based on 16S–23S rRNA gene internal transcribed spacer sequences. *J Clin Microbiol* **36**: 139–147.

Shepard CC (1960) The experimental diseases that follows the injection of human leprosy bacilli into foot-pads of mice. *J Exp Med* **112**: 445–454.

Springer B, Stockman L, Teschner K, Roberts GD & Bottger EC (1996) Two-laboratory collaborative study on identification of mycobacteria: molecular versus phenotypic methods. *J Clin Microbiol* **34**: 296–303.

Taylor TB, Patterson C, Hale Y & Safranek WW (1997) Routine use of PCR-restriction fragment length polymorphism analysis for identification of mycobacteria growing in liquid media. *J Clin Microbiol* **35**: 79–85.

Telenti A, Marchesi F, Balz M, Bally F, Bottger EC & Bodmer T (1993) Rapid identification of mycobacteria to the species level by polymerase chain reaction and restriction enzyme analysis. *J Clin Microbiol* **31**: 175–178.

Thai HTC, Le MQ, Vuong CD, Parida M, Minekawa H, Notomi T, Hasebe F & Morita K (2004) Development and evaluation of a novel loop-mediated isothermal amplification method for rapid detection of severe acute respiratory syndrome coronavirus. *J Clin Microbiol* **42**: 1956–1961.

Thompson JD, Higgins DG & Gibson TJ (1994) CLUSTAL W: improving the sensitivity of progressive multiple sequence alignment through sequence weighting, position-specific gap penalties and weight matrix choice. *Nucleic Acids Res* **22**: 4673–4680.

Turenne CY, Tschetter L, Wolfe J & Kabani A (2001) Necessity of quality-controlled 16S rRNA gene sequence databases: identifying nontuberculous *Mycobacterium* species. *J Clin Microbiol* **39**: 3637–3648.

Wayne LG & Sramek HA (1992) Agents of newly recognized or infrequently encountered mycobacterial diseases. *Clin Microbiol Rev* **5**: 1–25.

Yang M, Ross BC & Dwyer B (1993) Isolation of a DNA probe for identification of *Mycobacterium kansasii*, including the genetic subgroup. *J Clin Microbiol* **31**: 2769–2772.

JOURNAL OF BACTERIOLOGY, Jan. 2006, p. 86–95 Vol. 188, No. 1
0021-9193/06/$08.00+0 doi:10.1128/JB.188.1.86–95.2006

Identification and Characterization of the Genes Involved in Glycosylation Pathways of Mycobacterial Glycopeptidolipid Biosynthesis

Yuji Miyamoto,[1] Tetsu Mukai,[1] Noboru Nakata,[1] Yumi Maeda,[1] Masanori Kai,[1] Takashi Naka,[2] Ikuya Yano,[2] and Masahiko Makino[1]*

Department of Microbiology, Leprosy Research Center, National Institute of Infectious Diseases, 4-2-1 Aobacho, Higashimurayama, Tokyo 189-0002, Japan,[1] and Japan BCG Central Laboratory, 3-1-5 Matsuyama, Kiyose, Tokyo 204-0022, Japan[2]

Received 2 August 2005/Accepted 10 October 2005

Glycopeptidolipids (GPLs) are major components present on the outer layers of the cell walls of several nontuberculous mycobacteria. GPLs are antigenic molecules and have variant oligosaccharides in mycobacteria such as *Mycobacterium avium*. In this study, we identified four genes (*gtf1*, *gtf2*, *gtf3*, and *gtf4*) in the genome of *Mycobacterium smegmatis*. These genes were independently inactivated by homologous recombination in *M. smegmatis*, and the structures of GPLs from each gene disruptant were analyzed. Thin-layer chromatography, gas chromatography–mass spectrometry, and matrix-assisted laser desorption ionization–time-of-flight mass spectrometry analyses revealed that the mutants Δgtf1 and Δgtf2 accumulated the fatty acyl-tetrapeptide core having *O*-methyl-rhamnose and 6-deoxy-talose as sugar residues, respectively. The mutant Δgtf4 possessed the same GPLs as the wild type, whereas the mutant Δgtf3 lacked two minor GPLs, consisting of 3-*O*-methyl-rhamnose attached to *O*-methyl-rhamnose of the fatty acyl-tetrapeptide core. These results indicate that the *gtf1* and *gtf2* genes are responsible for the early glycosylation steps of GPL biosynthesis and the *gtf3* gene is involved in transferring a rhamnose residue not to 6-deoxy-talose but to an *O*-methyl-rhamnose residue. Moreover, a complementation experiment showed that *M. avium gtfA* and *gtfB*, which are deduced glycosyltransferase genes of GPL biosynthesis, restore complete GPL production in the mutants Δgtf1 and Δgtf2, respectively. Our findings propose that both *M. smegmatis* and *M. avium* have the common glycosylation pathway in the early steps of GPL biosynthesis but differ at the later stages.

The mycobacterial cell envelope has a unique structure that contains a complex of covalently linked peptidoglycan, arabinogalactan, and mycolic acids (7, 11). The outer layer of the cell envelope is composed of several types of glycolipids that affect the surface properties of mycobacterial cells (7, 11). Glycopeptidolipids (GPLs) are a major class of glycolipid present on the outer layer of several species of nontuberculous mycobacteria, such as *Mycobacterium avium* complex, *M. scrofulaceum*, *M. chelonae*, *M. fortuitum*, and *M. smegmatis* (31). GPLs have a common fatty acyl-tetrapeptide core consisting of tetrapeptide amino alcohol (D-Phe-D-*allo*-Thr-D-Ala-L-alaninol) and amide-linked long-chain fatty acid (C_{26-34}). The fatty acyl-tetrapeptide core is glycosylated with 6-deoxy-talose (6-d-Tal) and variable *O*-methyl-rhamnose (*O*-Me-Rha) residues, termed non-serovar-specific GPLs (nsGPLs), which are also the main products of *M. smegmatis* GPLs (1, 4, 10). The GPLs of *M. avium* have a more complicated structure, in which an additional Rha residue is added to 6-d-Tal of nsGPLs to be extended with various haptenic oligosaccharides, which are important surface antigens, resulting in serovar-specific GPLs (ssGPLs) (1, 4, 31).

There are some evidences that GPLs may be responsible for pathogenicity. It has been shown that the some of the ssGPLs are immunosuppressive and are able to induce a variety of cytokines, which affect host responses to infection (3, 15, 18, 29). Also, ssGPLs are identified as the factors modulating the phagocytosis and phagosome-lysosome fusion (17, 21). The altered GPL structure is also known to affect the colony morphology relevant to variable virulence (14, 30).

The biosyntheses of GPLs, particularly nsGPLs, have been characterized for *M. smegmatis*. Several biosynthetic genes encoding enzymes such as *O*-methyltransferase, acetyltransferase, and peptide synthetase have been identified (5, 16, 25, 26), but less is known about the genes involved in the glycosylation steps of the GPLs. The only glycosyltransferase gene that has been characterized is *rtfA* from *M. avium*, which is responsible for transferring the Rha residue to 6-d-Tal of nsGPLs to form ssGPLs (12). However, the initial glycosylation steps for the formation of nsGPLs remain unknown. Recently, it was shown that GPLs from *M. smegmatis* has a unique structure in which nsGPLs are further glycosylated, unlike ssGPLs (23, 24, 32), but these unique GPLs are produced in a carbon-starved situation, which is not a normal growth condition.

In this study, to clarify the glycosylation step leading to the formation of nsGPLs and its further products, we focused on four of the *M. smegmatis* genes having high similarity to *M. avium rtfA*, whose functions remain uncharacterized. Here, we have undertaken the gene disruption approach for generating each mutant in *M. smegmatis*, characterized their biochemical phenotypes, and finally hypothesized new biosynthetic pathways associated with glycosylation of GPLs.

* Corresponding author. Mailing address: Department of Microbiology, Leprosy Research Center, National Institute of Infectious Diseases, 4-2-1 Aobacho, Higashimurayama, Tokyo 189-0002, Japan. Phone: 81-42-391-8059. Fax: 81-42-391-8212. E-mail: mmaki@nih.go.jp.

TABLE 1. Bacterial strains and vectors used in this study

Strain or vector	Characteristic(s)	Source or reference
Bacteria		
E. coli		
DH5α	Cloning host	
STBL2	Cloning host	
M. smegmatis		
mc^2155	Wild type	27
Δgtf1	*gtf1* disruptant	This study
Δgtf2	*gtf2* disruptant	This study
Δgtf3	*gtf3* disruptant	This study
Δgtf4	*gtf4* disruptant	This study
M. avium		
JATA51-01 (ATCC 25291)	Source of *gtfA* and *gtfB*	
Vectors		
pYUB854	Cosmid vector	2
phAE87	Phasmid vector carrying full-length DNA of mycobacteriophage PH101	2
pMV261	*E. coli-Mycobacterium* shuttle vector carrying *hsp60* promoter cassette	28
pYUBgtf1	pYUB854 with *gtf1*-disrupted sequences for generating recombinant mycobacteriophage	This study
pYUBgtf2	pYUB854 with *gtf2*-disrupted sequences for generating recombinant mycobacteriophage	This study
pYUBgtf3	pYUB854 with *gtf3*-disrupted sequences for generating recombinant mycobacteriophage	This study
pYUBgtf4	pYUB854 with *gtf4*-disrupted sequences for generating recombinant mycobacteriophage	This study
pMVgtf1	pMV261 with *gtf1*	This study
pMVgtf2	pMV261 with *gtf2*	This study
pMVgtf3	pMV261 with *gtf3*	This study
pMVgtf4	pMV261 with *gtf4*	This study
pMVgtfA	pMV261 with *gtfA*	This study
pMVgtfB	pMV261 with *gtfB*	This study

MATERIALS AND METHODS

Bacterial strains, culture conditions, and DNA manipulation. Bacterial strains and vectors used and constructed are listed in Table 1. Mycobacterial strains for DNA manipulation were grown in Middlebrook 7H9 broth (Difco) with 0.05% Tween 80 or Middlebrook 7H10 agar (Difco) with 0.5% glycerol, and each was supplemented with 10% albumin-dextrose-catalase enrichment (Difco). *M. smegmatis* strains for GPL production were cultured in Luria-Bertani (LB) broth with 0.05% Tween 80. DNA manipulation including isolation of DNA, transformation, and PCR was carried out as described previously (22). *E. coli* strain DH5α was used for routine manipulation and propagation of plasmid DNA. *E. coli* strain STBL2 was used for construction of phasmid vectors derived from phAE87. Antibiotics was added as required: kanamycin, 50 μg/ml for *E. coli* and 25 μg/ml for *M. smegmatis*; hygromycin B, 150 μg/ml for *E. coli* and 75 μg/ml for *M. smegmatis*.

Generation of the gene disruptants. The targeted genes (*gtf1*, *gtf2*, *gtf3*, and *gtf4*) were selected by BLAST analysis of unfinished *M. smegmatis* genome sequences deposited in the database of The Institute for Genomic Research (TIGR) (http://www.tigr.org) with the *rfA* gene of *M. avium* as the query nucleotide sequence. Each gene was inactivated by inserting a hygromycin-resistant cassette (*hyg*) using the specialized transducing phage system (2). To construct the disrupted sequences, around 1.0-kb fragments both upstream and downstream of each gene were amplified from *M. smegmatis* mc^2155 genomic DNA using the following two pairs of primers: US1 and UA1 for upstream of *gtf1* and DS1 and DA1 for downstream of *gtf1*; US2 and UA2 for upstream of *gtf2* and DS2 and DA2 for downstream of *gtf2*; US3 and UA3 for upstream of *gtf3* and DS3 and DA3 for downstream of *gtf3*; US4 and UA4 for upstream of *gtf4* and DS4 and DA4 for downstream of *gtf4*. The PCR products were digested with each restriction enzyme and cloned into the corresponding sites flanking *hyg* of pYUB854 to give pYUBgtf1 (*gtf1*), pYUBgtf1 (*gtf2*), pYUBgtf3 (*gtf3*), and pYUBgtf4 (*gtf4*). These plasmids were used for packaging into the phasmid vector phAE87 to construct a specialized transducing mycobacteriophage for gene disruption as described previously (2). The *M. smegmatis* mc^2155 strain infected with the above mycobacteriophage at a multiplicity of infection of 10 was incubated at 37°C for 3 h in 7H9 broth without Tween 80. Harvested bacterial cells were then plated and cultured on 7H10 agar containing 75 μg/ml hygromycin B for 1 week. The hygromycin B-resistant colonies were selected, and their genomic DNA was subjected to PCR analysis to confirm the disruption of each gene using the following primers: U1 and D1 for *gtf1*; U2 and D2 for *gtf2*; U3 and D3 for *gtf3*; and U4 and D4 for *gtf4* (Fig. 1A to D).

Construction of the *gtf* expression vectors. The *gtf* genes of *M. smegmatis* and *M. avium* were amplified from each genomic DNA using the following primers: GTF1S and GTF1A for *gtf1*, GTF2S and GTF2A for *gtf2*, GTF3S and GTF3A for *gtf3*, GTF4S and GTF4A for *gtf4*, GTFAS and GTFAA for *gtfA*, and GTFBS and GTFBA for *gtfB*. The PCR products were digested with each restriction enzyme and cloned into the corresponding site of pMV261 to give pMVgtf1 (for the *gtf1* gene), pMVgtf2 (for the *gtf2* gene), pMVgtf3 (for the *gtf3* gene), pMVgtf4 (for the *gtf4* gene), pMVgtfA (for the *gtfA* gene), and pMVgtfB (for the *gtfB* gene). These vectors were used for complementation and overexpression experiment.

Isolation and purification of GPLs. The total lipids were extracted from harvested bacterial cells with $CHCl_3/CH_3OH$ (2:1, vol/vol) for several hours at room temperature. The extracts from the organic phase were separated from the aqueous phase and evaporated to dryness. For isolation of crude deacylated GPLs, total lipid fractions were subjected to mild alkaline hydrolysis as previously described (22, 25). For analytical thin-layer chromatography (TLC), the total lipid fraction after mild alkaline hydrolysis was spotted on silica gel 60 plates (Merck) and developed in $CHCl_3$-CH_3OH (9:1 [vol/vol]). Deacylated GPLs and other compounds were visualized by spraying with 10% H_2SO_4 and charring. Each total lipid fraction was extracted from an equal weight of harvested cells. Purified deacylated GPLs were separated from the total lipid fraction after mild alkaline hydrolysis by preparative TLC on the same plates and extracted from the bands corresponding to each GPLs. β-Elimination and perdeuteriomethylation treatment for determination of the linkage positions of sugar moieties were carried out as described previously (6, 9, 12).

GC/MS analysis. For monosaccharide analysis, purified deacylated GPLs or total lipid fraction after mild alkaline hydrolysis was hydrolyzed in 2 M trifluoroacetic acid (2 h, 120°C), and released sugars from deacylated GPLs were reduced with $NaBD_4$ (sodium borodeuteride) and then acetylated with pyridine-acetic anhydride (1:1 [vol/vol]) at room temperature overnight. Each total lipid fraction was extracted from an equal weight of harvested cells. The resulting

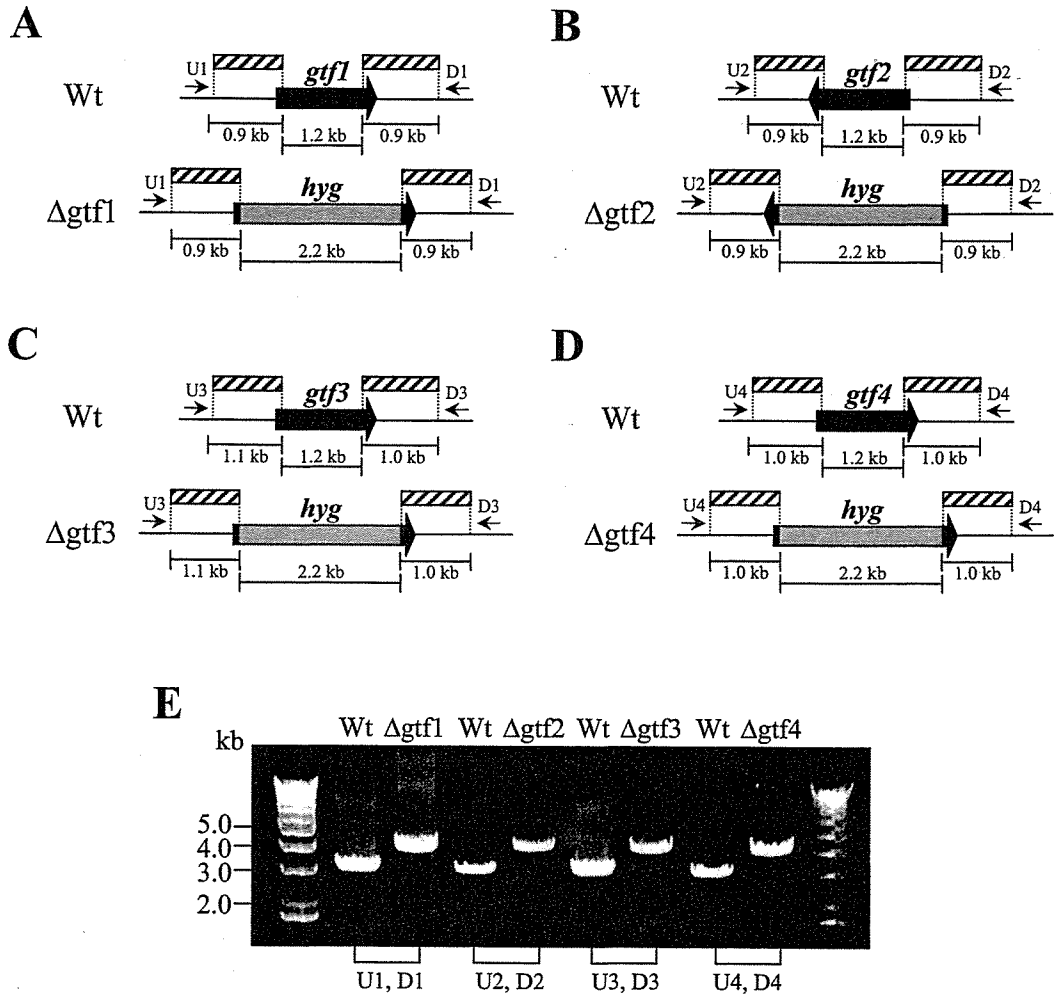

FIG. 1. Generation of *gtf* gene disruptants. (A to D) Schematic diagram of each *gtf* region on the chromosome of the wild-type *M. smegmatis* mc^{2}155 strain (Wt) and its gene disruptants Δgtf1, Δgtf2, Δgtf3, and Δgtf4. The shaded boxes indicate the regions included in recombinant phage for gene disruption. The black arrows represent the coding region of each *gtf* gene. The gray boxes represent the hygromycin resistance cassette (*hyg*). The primers used for PCR analysis are indicated by small arrows. (E) PCR analyses of the wild type and each disruptant using the primers indicated above.

alditol acetates were separated and analyzed by gas chromatography–mass spectrometry (GC/MS) on TRACE DSQ (Thermo electron) instrument equipped with an SP-2380 column (SUPELCO) using helium gas. The temperature program was from 52 to 172°C at 40°C/min and then 172 to 250°C at 3°C/min.

MALDI-TOF/MS analysis. To determine the total mass of the purified deacylated GPLs, matrix-assisted laser desorption ionization–time-of-flight (MALDI-TOF) mass spectra (in the positive mode) were acquired on a QSTAR XL (Applied Biosystems) with a pulse laser emitting at 337 nm. Samples mixed with 2,5-dihydroxybenzoic acid as the matrix were analyzed in the reflectron mode with an accelerating voltage operating in positive ion mode of 20 kV.

RESULTS

Disruption of *gtf1*, *gtf2*, *gtf3*, and *gtf4* by allelic exchange. Four genes showing high similarity to the *rtfA* gene, involved in GPL biosynthesis of *M. avium*, were identified for the *M. smegmatis* mc^{2}155 strain (12). The homologies of their corresponding amino acid sequences with that of RtfA were around 60%. Three genes were found in the GPL biosynthetic gene cluster, namely, *gtf1*, *gtf2*, and *gtf3* (GenBank accession no. AY138899.1) (16), whereas one gene, designated *gtf4* (TIGR database no. 4839918 to 4841162), was located far from the other three genes. To examine whether these genes are responsible for GPL biosynthesis, we generated four gene disruptants, designated Δgtf1, Δgtf2, Δgtf3, and Δgtf4, using the specialized transducing mycobacteriophage containing the entire open reading frame, replacing with the hygromycin resistance cassette (2). For confirmation of the gene disruption, PCR analysis was performed on chromosomal DNA from each disruptant. To avoid the amplification of disrupted sequences derived from residual mycobacteriophage, we designed and used the primers located outside the sequences included in each mycobacteriophage as shown in Fig. 1A to D. As expected, around 3.0-kb fragments were amplified from mc^{2}155 (wild type), whereas around 4.0-kb fragments were amplified from each disruptant, because most of the *gtf* coding region (1.2 kb) was replaced by the hygromycin resistance cassette (2.2 kb) (Fig. 1E). These results demonstrated that allelic exchanges involving replacement of the *gtf* genes with the disrupted constructs have been successful.

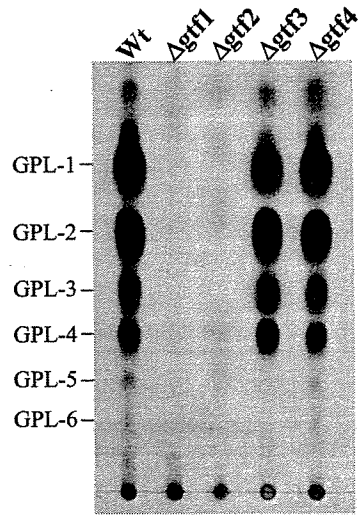

FIG. 2. TLC analyses of crude GPL extracts from the *M. smegmatis* mc^2155 strain (Wt) and its gene disruptants. The total lipid fraction after mild alkaline hydrolysis was spotted on plates and developed in $CHCl_3$-CH_3OH (9:1 [vol/vol]). GPLs were visualized by spraying with 10% H_2SO_4 and charring. Each total lipid fraction was extracted from an equal weight of harvested cells.

TLC analysis of gene disruptants. To investigate the effects of the mutation in each *gtf* gene, we examined GPL production of four gene disruptants. TLC analyses of total lipid fraction after mild alkaline hydrolysis revealed that wild-type mc^2155 mainly produced six components, designated GPL-1 to -6, whereas Δgtf1 and Δgtf2 lacked all six components and Δgtf3 lacked two minor ones (GPL-5 and GPL-6) found in the wild type (Fig. 2). In contrast, no differences in TLC profile were observed between Δgtf4 and the wild type (Fig. 2).

Characterization of Δgtf1 and Δgtf2. In Δgtf1 and Δgtf2, the TLC analyses showed that six GPL components contained in the wild type had disappeared. On the other hand, there is the possibility that both disruptants contained GPL derivatives which are structurally incomplete and hard to be detected by TLC analyses. To characterize the sugars included in GPL derivatives from both disruptants and to compare with the wild type, each total lipid fraction after mild alkaline hydrolysis was hydrolyzed, and the released monosaccharides as their alditol acetates were examined by GC/MS. Figure 3 shows that the profiles of the wild type gave three peaks corresponding to 2,3,4-tri-*O*-Me-Rha, 3,4-di-*O*-Me-Rha, and 6-d-Tal (Fig. 3A), whereas Δgtf1 lacked 6-d-Tal (Fig. 3B) and Δgtf2 lacked 3,4-di-*O*-Me-Rha and 2,3,4-tri-*O*-Me-Rha (Fig. 3C). Complementation of both disruptants with each respective gene restored the TLC profile of GPLs to that observed for the wild type (not shown). Therefore, the *gtf1* and *gtf2* genes are found to be responsible for transferring the 6-d-Tal and Rha residues, respectively.

Structural determination of GPL-5 and GPL-6 for characterization of Δgtf3. The TLC profile of Δgtf3 showed that two spots (GPL-5 and GPL-6) disappeared (Fig. 2). To reveal the biosynthetic role of the *gtf3* gene, GPL-5 and GPL-6 were purified from mc^2155 and their structures were determined. GC/MS analyses showed that GPL-5 and GPL-6 contained 6-d-Tal and 3,4-di-*O*-Me-Rha, which were identified as sugar

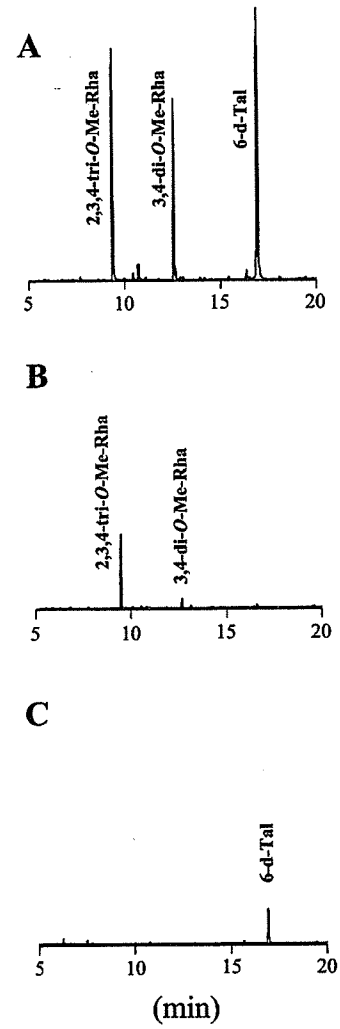

FIG. 3. GC/MS analyses of alditol acetates of sugars released from crude GPLs. GPLs were extracted from *M. smegmatis* strains: (A) mc^2155 strain, (B) Δgtf1, and (C) Δgtf2. Alditol acetate derivatives were prepared from the total lipid fraction after mild alkaline hydrolysis, which was extracted from an equal weight of harvested cells.

moieties of GPL-3 and GPL-4 (Fig. 4A). However, an extra sugar, 3-*O*-Me-Rha, was also detected (Fig. 4A). MALDI-TOF/MS analyses revealed that the main molecular ions of GPL-5 (*m/z* 1,333.8) and GPL-6 (*m/z* 1,319.8) were 160 mass units higher than those of GPL-3 (*m/z* 1,173.9) and GPL-4 (*m/z* 1,159.9), respectively (Fig. 4B). These results confirmed the presence of 3-*O*-Me-Rha in GPL-5 and GPL-6 and also suggested that 3-*O*-Me-Rha was further added to GPL-3 and GPL-4. Although GPL-5 and GPL-6 contained same three sugars, the spectra showed that the main molecular ion of GPL-5 (*m/z* 1,333.8) was 14 mass units higher than that of GPL-6 (*m/z* 1,319.8) (Fig. 4Ba and 4Bb). These differences in total mass may be due to O methylation of fatty acid as observed in structures of GPL-1 and GPL-3, suggesting that fatty acid of GPL-5 was O methylated like GPL-1 and GPL-3 (16). To investigate the sugar linked to D-*allo*-Thr of the fatty acyl-tetrapeptide core, GPL-5 and GPL-6 were subjected to β-elimination treatment. The main ion peaks of treated GPL-5 and

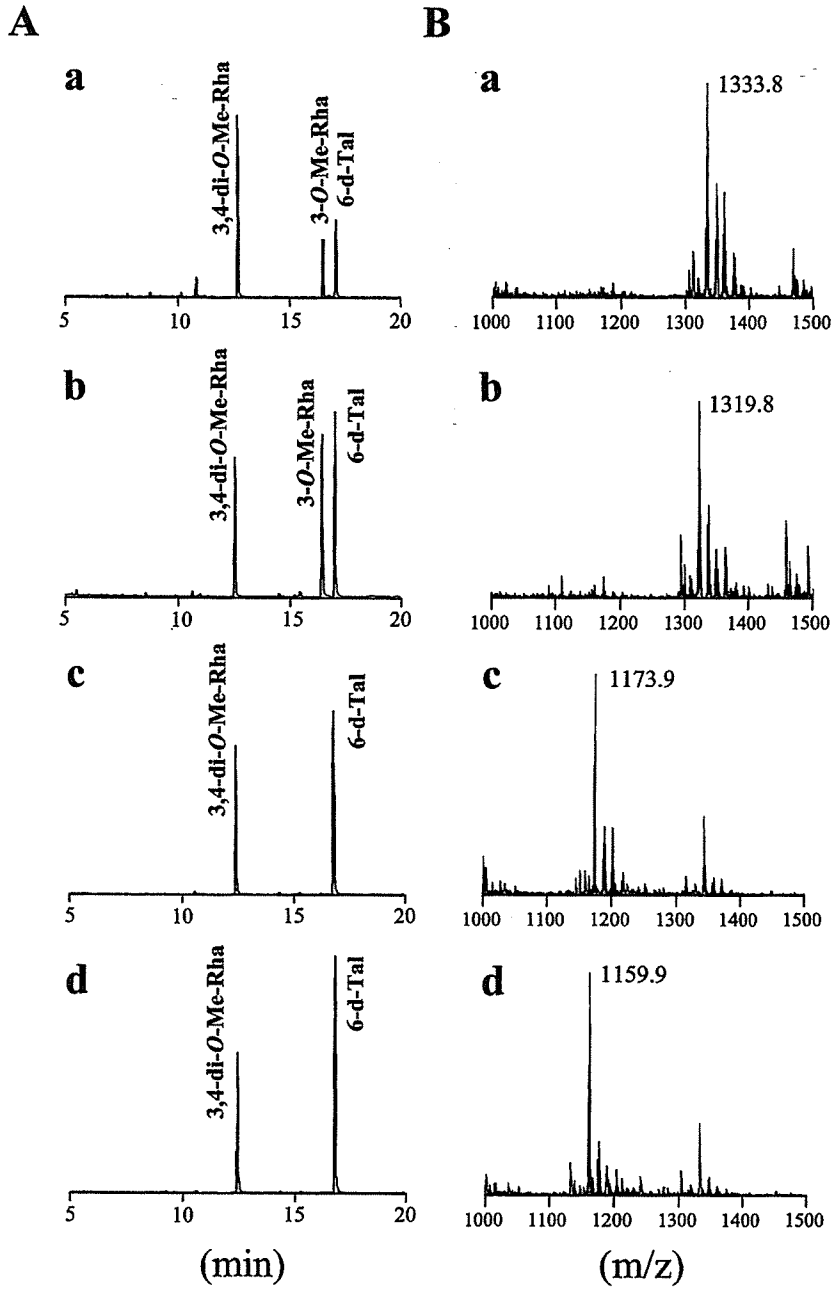

FIG. 4. Biochemical characterization of GPL-5 (a), GPL-6 (b), GPL-3 (c), and GPL-4 (d). (A) GC/MS analysis of alditol acetates of sugars released from each purified GPL. (B) MALDI-TOF/MS analysis of total molecular mass of each purified GPLs. (C) MALDI-TOF/MS analysis of total molecular mass of purified GPL-5 (a) and GPL-6 (b), which were subjected to β-elimination.

GPL-6 were *m/z* 1,171.7 and 1,157.7, respectively, which resulted in the loss of total mass of 162, suggesting that 6-d-Tal was linked to the position of D-*allo*-Thr (Fig. 4C). The linkage position of the sugars linked to the L-alaninol site of GPL-5 and GPL-6 was then determined by GC/MS analyses followed by perdeuteriomethylation. As shown in Fig. 5A, the GC profiles of alditol acetates from perdeuteriomethylated GPL-5 gave three peaks corresponding to 6-d-Tal, 3-*O*-Me-Rha, and 3,4-di-*O*-Me-Rha. The characteristic spectra of 3-*O*-Me-Rha and 3,4-di-*O*-Me-Rha, which are predicted to be linked to L-alaninol, are illustrated in Fig. 5B and C, respectively. The spectrum of 3-*O*-Me-Rha gave fragment ions at *m/z* 121, 134, and 165, which represent the presence of a deuteriomethyl group at positions C-2 and C-4. In contrast, no deuteriomethyl group was observed in 3,4-di-*O*-Me-Rha, whose C-2 position was acetylated, supported by the detection of fragment ions at *m/z* 131 and 190. The results from GC/MS analyses of perdeuteriomethylated GPL-6 were the same as those for GPL-5 (not shown). These observations demonstrated that GPL-5 and GPL-6 have the same sugar moieties, which are 6-d-Tal at

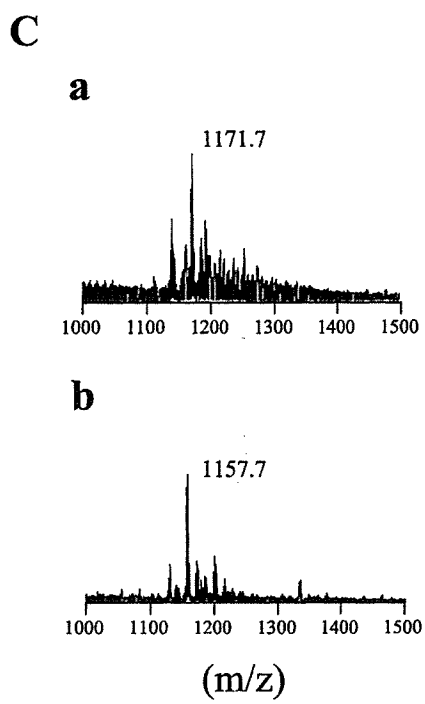

FIG. 4—*Continued.*

D-*allo*-Thr and 3-*O*-Me-rhamnosyl-(1→2)-3,4-di-*O*-Me-Rha at L-alaninol, indicating that 3-*O*-Me-Rha was linked to GPL-3 and GPL-4 (Fig. 6).

Overexpression of *gtf1*, *gtf2*, *gtf3*, and *gtf4* in *M. smegmatis* mc^{2}155. To investigate the effects of overexpression of each gene on GPL biosynthesis, we constructed four *gtf*-overexpressed strains in wild-type mc^{2}155 and compared the profile of total GPLs by TLC analyses. The results showed that the profiles of Wt/pMVgtf1, Wt/pMVgtf2, and Wt/pMVgtf4 were the same as that of Wt/pMV261, whereas Wt/pMVgtf3 produced two major compounds whose biochemical data corresponded to those of GPL-5 and GPL-6 (Fig. 7).

Characterization of *M. avium gtfA* and *gtfB*. We showed that both *M. smegmatis gtf1* and *gtf2* were responsible for glycosylation of the fatty acyl-tetrapeptide core. Comparison of the genome sequences encompassing the GPL biosynthetic gene cluster among several species of *M. avium* have shown that *gtfA* and *gtfB* (GenBank accession no. AF125999.1) are very similar to *M. smegmatis gtf1* and *gtf2*, respectively, in the corresponding putative amino acid sequences and might contribute to the glycosylation of the fatty acyl-tetrapeptide core (13). However, the function of each gene has not been thoroughly analyzed (13). Therefore, to confirm the role of *gtfA* and *gtfB*, we complemented Δgtf1 and Δgtf2 with the *gtf* expression vectors carrying *gtfA* (pMVgtfA) and *gtfB* (pMVgtfB). As shown in Fig. 8, TLC analyses revealed that *gtfA* and *gtfB* restored the production of wild-type GPLs in Δgtf1 and Δgtf2, respectively, whereas transformants with reverse vectors (Δgtf1/pMVgtfB and Δgtf2/pMVgtfA) did not produce wild-type GPLs. These results suggested that the function of *M. avium gtfA* and *gtfB* is the same as that of *M. smegmatis gtf1* and *gtf2*, respectively.

DISCUSSION

It has been shown that the *rtfA* gene of *M. avium* encodes a rhamnosyltransferase which synthesizes ssGPLs, while other genes involved in the glycosylation of the fatty acyl-tetrapeptide core remain unknown (12). In this study, we focused on the four genes of *M. smegmatis*, which show high similarity to *rtfA*, and generated their disruptants to characterize the role in the GPL biosynthesis.

In the early glycosylation steps of the fatty acyl-tetrapeptide core, we observed that the disruption of *gtf1* abolished the whole GPLs and led to the accumulation of *O*-Me-Rha derivatives without 6-d-Tal in Δgtf1 (Fig. 3B). Thus, we propose that the *gtf1* gene product catalyzes the transfer of 6-d-Tal to fatty acyl-tetrapeptide core. It is reported that the *M. avium* 104Rg strain, which has a spontaneous deletion in the genome region including *gtfA*, also accumulated *O*-methylated and nonmethylated Rha without 6-d-Tal (13, 30). This property is directly supported by our result that the *gtfA* could complement Δgtf1 (Fig. 8). However, *M. avium* 104Rg mainly contained nonmethylated Rha, whereas Δgtf1 derived from *M. smegmatis* mc^{2}155 contained only *O*-Me-Rha. These different observations may be due to differences in the substrate specificity of methyltransferase, because 2,3,4-tri-*O*-Me-Rha was present in *M. smegmatis* mc^{2}155 but was not identified in *M. avium* species (8, 25).

When the *gtf2* gene was disrupted, we detected 6-d-Tal without Rha derivatives in GC/MS analysis, which demonstrates that the *gtf2* gene contributes to the transfer of Rha to the fatty acyl-tetrapeptide core (Fig. 3C). In addition, complementation revealed that the *gtfB* gene of *M. avium* had the same function as *gtf2* (Fig. 8). In the previous studies of GPL biosyntheses, the mutant accumulating 6-d-Tal-containing derivatives without the Rha residue have not been isolated from GPL-producing species so far. Our results directly indicated for the first time that 6-d-Tal-containing derivatives could be an intermediate for the biosynthetic pathways of GPLs.

As for the order of glycosylation steps regulated by *gtf1* and *gtf2*, we cannot determine which step takes place earlier, since both disruptants accumulated the intermediates having different component (Fig. 3B and C). For *M. avium* serovar 2, Eckstein et al. proposed a pathway in which the transfer of the Rha residue to the fatty acyl-tetrapeptide core occurred prior to that of 6-d-Tal, because a mutant strain, 104Rg, having the *gtfA* region deleted, accumulated the fatty acyl-tetrapeptide core with only the Rha residue (13). However, our results lead to the interesting possibility that there are two alternative glycosylation pathways for the formation of nsGPLs (Fig. 9). If the glycosylation should occur in a single pathway, we would expect the accumulation of a nonglycosylated intermediate in either of the disruptants, because one of the genes, *gtf1* or *gtf2*, would be responsible for the first step of glycosylation converting the fatty acyl-tetrapeptide core to a glycosylated intermediate. Thus, the detection of glycosylated intermediates from both Δgtf1 and Δgtf2 suggests that (i) the fatty acyl-tetrapeptide core could be the substrate for both Gtf1 and Gtf2 and (ii) the glycosylated intermediates could also be the substrates for both Gtf1 and Gtf2. We prove here that Gtf1 and Gtf2 have broad substrate specificity and propose that the fatty acyl-tetrapeptide core is glycosylated by Gtf1 and Gtf2 at the same

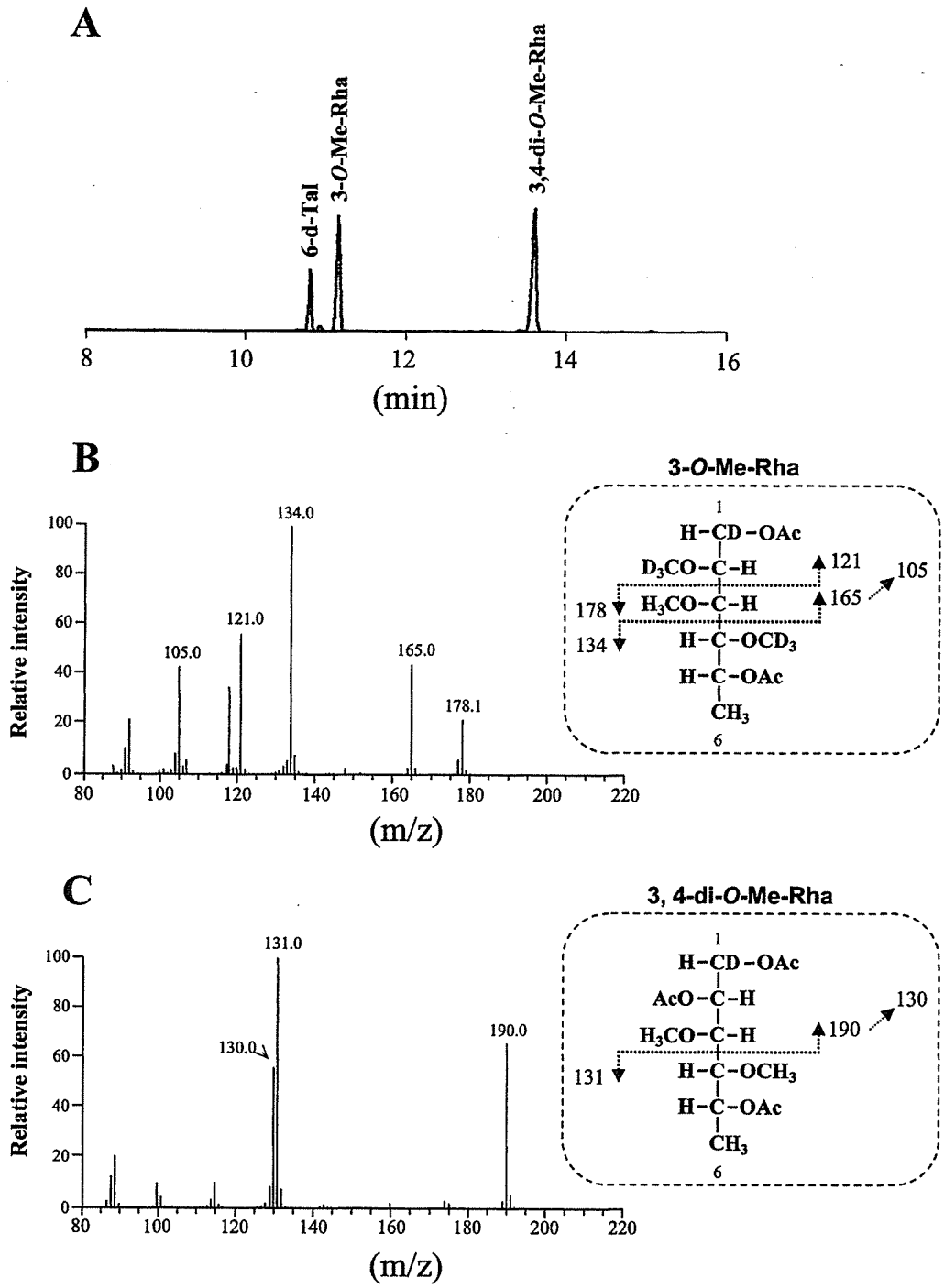

FIG. 5. GC/MS analysis of alditol acetates of sugars released from perdeuteriomethylated GPL-5. (A) GC profile. (B) Mass spectrum and fragment ion assignment corresponding to 3-*O*-Me-Rha. (C) Mass spectrum of fragment ion assignment corresponding to 3,4-di-*O*-Me-Rha.

time and then converted to the nsGPLs having both 6-d-Tal and *O*-Me-Rha via cross-glycosylations (Fig. 9).

Structural determination of GPL-5 and GPL-6 revealed that L-alaninol of the fatty acyl-tetrapeptide core was glycosylated with disaccharide (3-*O*-Me- and 3,4-di-*O*-Me-Rha), which was structurally different from GPLs including GPL-1 to -4 and ssGPLs (Fig. 6). However, it is reported that *M. fortuitum* complex produced GPLs which are glycosylated as in GPL-5 and GPL-6 as major components (19, 20). Therefore, these observations suggest that this type of glycosylation is not specific for *M. smegmatis*. GC/MS analyses of GPL-5 and GPL-6 indicated the presence of 3-*O*-Me-Rha in addition to 3,4-di-*O*-Me-Rha, and analyses of perdeuteriomethylated GPL-5 and GPL-6 showed that position C-1 of 3-*O*-Me-Rha is linked to position C-2 of 3,4-di-*O*-Me-Rha. Recent studies have shown that *M. smegmatis* mc^2155 newly produces two polar GPLs

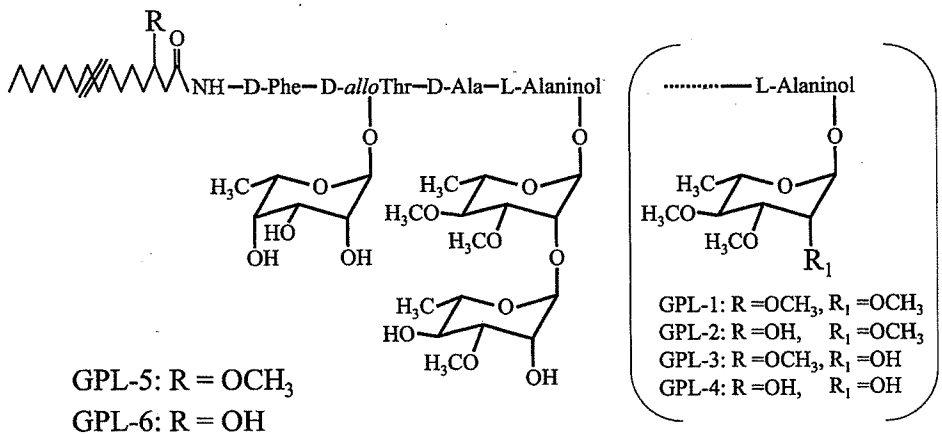

FIG. 6. Proposed structures of GPL-5 and GPL-6. Figure in parentheses shows the structure of GPL-1, GPL-2, GPL-3, and GPL-4, which were characterized in previous studies (10, 16, 25).

which contained two units of 3,4-di-*O*-Me-Rha at L-alaninol of the fatty acyl-tetrapeptide core with no 3-*O*-Me-Rha at any other position when cultured in carbon-limited medium (23, 24). However, the reason for not being able to detect 3-*O*-Me-Rha remains unknown.

In the *gtf3*-overexpressed strain Wt/pMVgtf3, the productivities of GPL-5 and GPL-6 were much higher than those of other GPLs (Fig. 7). So, we can speculate that the expression level of *gtf3* is usually repressed and could be regulated by some environmental factors, such as the nutrient condition or the gene encoding sigma factor (23, 24). GC/MS analyses showed that GPL-5 and GPL-6 have the structures in which 3-*O*-Me-Rha is linked to GPL-3 and GPL-4. These results suggest that GPL-3 and GPL-4 could be the precursors of GPL-5 and GPL-6, respectively, and in Wt/pMVgtf3, overexpression of *gtf3* resulted in 2-*O*-rhamnosylation of 3,4-di-*O*-Me-Rha in GPL-3 and GPL-4 instead of 2-*O*-methylation for converting to GPL-1 and GPL-2, so that GPL-5 and GPL-6 were synthesized.

Figure 9 represents proposed glycosylation steps related to *M. smegmatis* and *M. avium*. We showed that the functions of *gtf1* and *gtf2* corresponded to those of *gtfA* and *gtfB*, respectively. This finding demonstrates that the biosynthetic pathway for nsGPLs, which is the glycosylation of the fatty acyl-tetrapeptide core with the 6-d-Tal and Rha residues, is common between *M. smegmatis* and *M. avium*. Moreover, the biochemical characterization of Δgtf2 and Δgtf1 suggested that the glycosylation pathways for nsGPLs might not be stringent. On the other hand, it has been shown that the *rtfA* gene of *M. avium* triggers the biosynthesis of ssGPLs by transfer of Rha to 6-d-Tal of nsGPLs (12). In *M. smegmatis*, our results indicated that the *gtf3* gene plays a role in synthesis of 3-*O*-Me-rhamno-

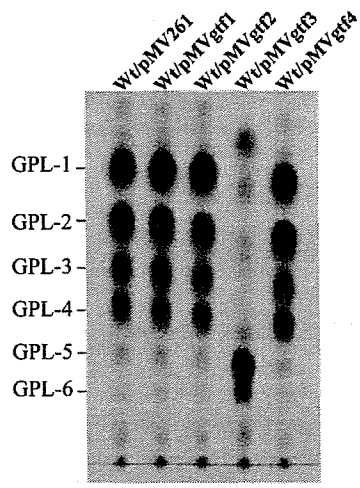

FIG. 7. TLC analyses of crude GPL extracts from the *M. smegmatis* mc^2155 strain (Wt) transformed with *gtf* expression vectors. Total lipid fraction after mild alkaline hydrolysis was spotted on plates and developed in $CHCl_3$-CH_3OH (9:1 [vol/vol]). GPLs were visualized by spraying with 10% H_2SO_4 and charring. Each total lipid fraction was extracted from an equal weight of harvested cells.

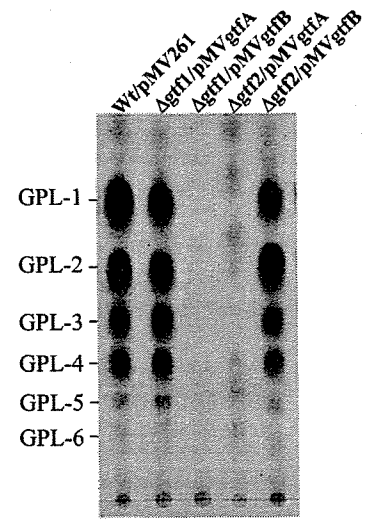

FIG. 8. TLC analyses of crude GPL extracts from the *M. smegmatis* mc^2155 strain (Wt) and its gene disruptants transformed with *M. avium* *gtfA* and *gtfB*. Total lipid fraction after mild alkaline hydrolysis was spotted on plates and developed in $CHCl_3$-CH_3OH (9:1 [vol/vol]). GPLs were visualized by spraying with 10% H_2SO_4 and charring. Each total lipid fraction was extracted from an equal weight of harvested cells.

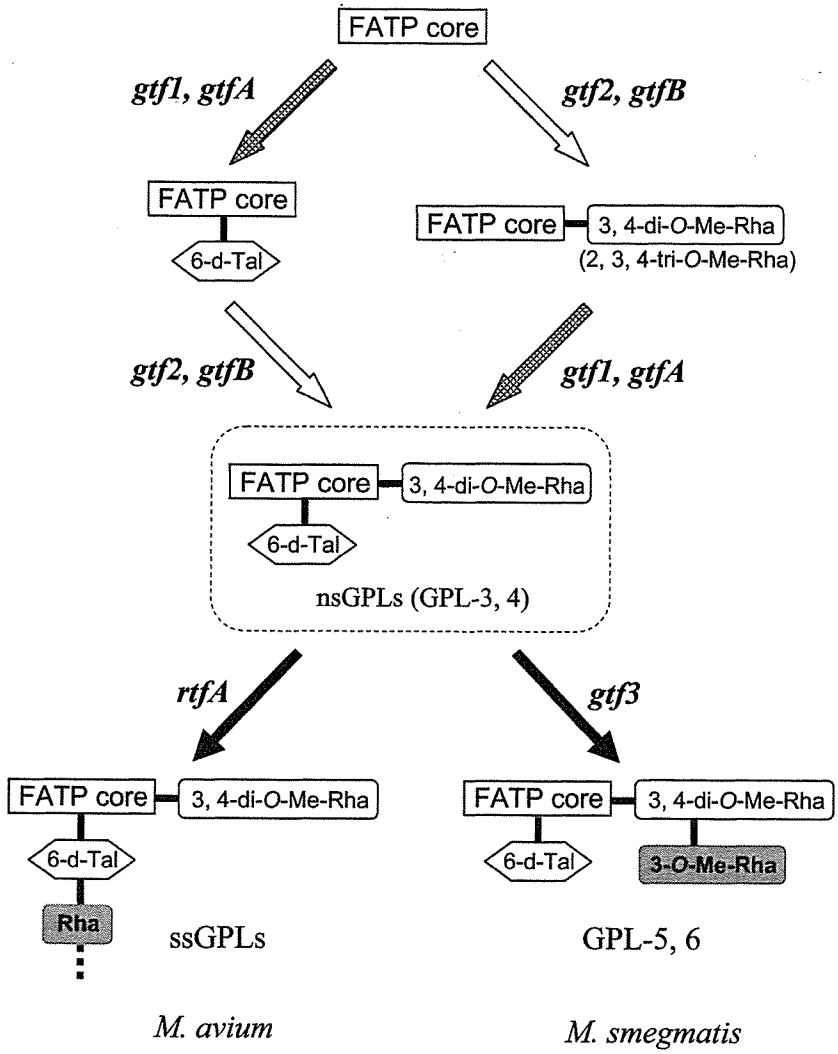

FIG. 9. Proposed biosynthetic pathways for GPLs of *M. smegmatis* and *M. avium*. FATP core, fatty acyl-tetrapeptide core.

syl-(1→2)-3,4-di-*O*-Me-Rha linked to L-alaninol of the fatty acyl-tetrapeptide core by transfer of an extra Rha residue to nsGPLs. Thus, the *rtfA* and *gtf3* genes have the ability to confer the biosynthetic differences between *M. avium* and *M. smegmatis*, suggesting that these genes may be responsible for the phylogenetic distinctions in the two species of mycobacteria.

ACKNOWLEDGMENTS

We thank W. R. Jacobs, Jr. (Albert Einstein College of Medicine, N.Y.), for providing us with the specialized transducing phage system.

This work was supported in part by grants from Health Science Research Grants—Research on Emerging and Re-emerging Infectious Diseases, Grant-in-Aid for Research on HIV/AIDS, the Ministry of Health, Labor and Welfare, Japan.

REFERENCES

1. **Aspinall, G. O., D. Chatterjee, and P. J. Brennan.** 1995. The variable surface glycolipids of mycobacteria: structures, synthesis of epitopes, and biological properties. Adv. Carbohydr. Chem. Biochem. **51:**169–242.
2. **Bardarov, S., S. Bardarov, Jr., M. S. Pavelka, Jr., V. Sambandamurthy, M. Larsen, J. Tufariello, J. Chan, G. Hatfull, and W. R. Jacobs, Jr.** 2002. Specialized transduction: an efficient method for generating marked and unmarked targeted gene disruptions in *Mycobacterium tuberculosis*, *M. bovis* BCG, and *M. smegmatis*. Microbiology **148:**3007–3017.
3. **Barrow, W. W., T. L. Davis, E. L. Wright, V. Labrousse, M. Bachelet, and N. Rastogi.** 1995. Immunomodulatory spectrum of lipids associated with *Mycobacterium avium* serovar 8. Infect. Immun. **63:**126–133.
4. **Belisle, J. T., K. Klaczkiewicz, P. J. Brennan, W. R. Jacobs, Jr., and J. M. Inamine.** 1993. Rough morphological variants of *Mycobacterium avium*. Characterization of genomic deletions resulting in the loss of glycopeptidolipid expression. J. Biol. Chem. **268:**10517–10523.
5. **Billman-Jacobe, H., M. J. McConville, R. E. Haites, S. Kovacevic, and R. L. Coppel.** 1999. Identification of a peptide synthetase involved in the biosynthesis of glycopeptidolipids of *Mycobacterium smegmatis*. Mol. Microbiol. **33:**1244–1253.
6. **Bjorndal, H., C. G. Hellerqvist, B. Lindberg, and S. Svensson.** 1970. Gas-liquid chromatography and mass spectrometry in methylation analysis of polysaccharides. Angew. Chem. Int. Ed. **9:**610–619.
7. **Brennan, P. J., and H. Nikaido.** 1995. The envelope of mycobacteria. Annu. Rev. Biochem. **64:**29–63.
8. **Chatterjee, D., and K. H. Khoo.** 2001. The surface glycopeptidolipids of mycobacteria: structures and biological properties. Cell. Mol. Life Sci. **58:** 2018–2042.
9. **Ciucanu, I., and F. Kerek.** 1984. A simple and rapid method for the permethylation of carbohydrates. Carbohydr. Res. **131:**209–217.
10. **Daffe, M., M. A. Laneelle, and G. Puzo.** 1983. Structural elucidation by field desorption and electron-impact mass spectrometry of the C-mycosides isolated from *Mycobacterium smegmatis*. Biochim. Biophys. Acta **751:**439–443.
11. **Daffe, M., and P. Draper.** 1998. The envelope layers of mycobacteria with reference to their pathogenicity. Adv. Microb. Physiol. **39:**131–203.
12. **Eckstein, T. M., F. S. Silbaq, D. Chatterjee, N. J. Kelly, P. J. Brennan, and J. T. Belisle.** 1998. Identification and recombinant expression of a *Mycobac-*

terium avium rhamnosyltransferase gene (*rtfA*) involved in glycopeptidolipid biosynthesis. J. Bacteriol. **180:**5567–5573.

13. **Eckstein, T. M., J. T. Belisle, and J. M. Inamine.** 2003. Proposed pathway for the biosynthesis of serovar-specific glycopeptidolipids in *Mycobacterium avium* serovar 2. Microbiology **149:**2797–2807.
14. **Etienne, G., C. Villeneuve, H. Billman-Jacobe, C. Astarie-Dequeker, M. A. Dupont, and M. Daffe.** 2002. The impact of the absence of glycopeptidolipids on the ultrastructure, cell surface and cell wall properties, and phagocytosis of *Mycobacterium smegmatis*. Microbiology **148:**3089–3100.
15. **Horgen, L., E. L. Barrow, W. W. Barrow, and N. Rastogi.** 2000. Exposure of human peripheral blood mononuclear cells to total lipids and serovar-specific glycopeptidolipids from *Mycobacterium.avium* serovars 4 and 8 results in inhibition of TH1-type responses. Microb. Pathog. **29:**9–16.
16. **Jeevarajah, D., J. H. Patterson, M. J. McConville, and H. Billman-Jacobe.** 2002. Modification of glycopeptidolipids by an *O*-methyltransferase of *Mycobacterium smegmatis*. Microbiology **148:**3079–3087.
17. **Kano, H., T. Doi, Y. Fujita, H. Takimoto, I. Yano, and Y. Kumazawa.** 2005. Serotype-specific modulation of human monocyte functions by glycopeptidolipid (GPL) isolated from *Mycobacterium avium* complex. Biol. Pharm. Bull. **28:**335–339.
18. **Krzywinska, E., S. Bhatnagar, L. Sweet, D. Chatterjee, and J. S. Schorey.** 2005. *Mycobacterium avium* 104 deleted of the methyltransferase D gene by allelic replacement lacks serotype-specific glycopeptidolipids and shows attenuated virulence in mice. Mol. Microbiol. **56:**1262–1273.
19. **Lopez Marin, L. M., M. A. Laneelle, D. Prome, M. Daffe, G. Laneelle, and J. C. Prome.** 1991. Glycopeptidolipids from *Mycobacterium fortuitum*: a variant in the structure of C-mycoside. Biochemistry **30:**10536–10542.
20. **Lopez-Marin, L. M., N. Gautier, M. A. Laneelle, G. Silve, and M. Daffe.** 1994. Structures of the glycopeptidolipid antigens of *Mycobacterium abscessus* and *Mycobacterium chelonae* and possible chemical basis of the serological cross-reactions in the *Mycobacterium fortuitum* complex. Microbiology **140:**1109–1118.
21. **Minami, H.** 1998. Promotion of phagocytosis and prevention of phagosome-lysosome (P-L) fusion in human peripheral blood monocytes by serotype specific glycopeptidolipid (GPL) antigen of *Mycobacterium avium* complex (MAC). Kekkaku **73:**545–556.
22. **Miyamoto, Y., T. Mukai, F. Takeshita, N. Nakata, Y. Maeda, M. Kai, and M. Makino.** 2004. Aggregation of mycobacteria caused by disruption of fibronectin-attachment protein-encoding gene. FEMS Microbiol. Lett. **236:** 227–234.
23. **Mukherjee, R., M. Gomez, N. Jayaraman, I. Smith, and D. Chatterji.** 2005. Hyperglycosylation of glycopeptidolipid of *Mycobacterium smegmatis* under nutrient starvation: structural studies. Microbiology **151:**2385–2392.
24. **Ojha, A. K., S. Varma, and D. Chatterji.** 2002. Synthesis of an unusual polar glycopeptidolipid in glucose-limited culture of *Mycobacterium smegmatis*. Microbiology **148:**3039–3048.
25. **Patterson, J. H., M. J. McConville, R. E. Haites, R. L. Coppel, and H. Billman-Jacobe.** 2000. Identification of a methyltransferase from *Mycobacterium smegmatis* involved in glycopeptidolipid synthesis. J. Biol. Chem. **275:**24900–24906.
26. **Recht, J., and R. Kolter.** 2001. Glycopeptidolipid acetylation affects sliding motility and biofilm formation in *Mycobacterium smegmatis*. J. Bacteriol. **183:**5718–5724.
27. **Snapper, S. B., R. E. Melton, S. Mustafa, T. Kieser, and W. R. Jacobs, Jr.** 1990. Isolation and characterization of efficient plasmid transformation mutants of *Mycobacterium smegmatis*. Mol. Microbiol. **4:**1911–1919.
28. **Stover, C. K., V. F. de la Cruz, T. R. Fuerst, J. E. Burlein, L. A. Benson, L. T. Bennett, G. P. Bansal, J. F. Young, M. H. Lee, G. F. Hatfull, S. B. Snapper, R. G. Barletta, W. R. Jacobs, Jr., and B. R. Bloom.** 1991. New use of BCG for recombinant vaccines. Nature **351:**456–460.
29. **Tassell, S. K., M. Pourshafie, E. L. Wright, M. G. Richmond, and W. W. Barrow.** 1992. Modified lymphocyte response to mitogens induced by the lipopeptide fragment derived from *Mycobacterium avium* serovar-specific glycopeptidolipids. Infect. Immun. **60:**706–711.
30. **Torrelles, J. B., D. Ellis, T. Osborne, A. Hoefer, I. M. Orme, D. Chatterjee, P. J. Brennan, and A. M. Cooper.** 2002. Characterization of virulence, colony morphotype and the glycopeptidolipid of *Mycobacterium avium* strain 104. Tuberculosis (Edinburgh) **82:**293–300.
31. **Vergne, I., and M. Daffe.** 1998. Interaction of mycobacterial glycolipids with host cells. Front. Biosci. **3:**d865–d876.
32. **Villeneuve, C., G. Etienne, V. Abadie, H. Montrozier, C. Bordier, F. Laval, M. Daffe, I. Maridonneau-Parini, and C. Astarie-Dequeker.** 2003. Surface-exposed glycopeptidolipids of *Mycobacterium smegmatis* specifically inhibit the phagocytosis of mycobacteria by human macrophages. Identification of a novel family of glycopeptidolipids. J. Biol. Chem. **278:**51291–51300.

Augmented induction of CD8$^+$ cytotoxic T-cell response and antitumour resistance by T helper type 1-inducing peptide

Takeshi Kikuchi,[1,2] Shuichiro Uehara,[1,2] Haruyuki Ariga,[1,3] Takeshi Tokunaga,[1] Ai Kariyone,[1] Toshiki Tamura[1] and Kiyoshi Takatsu[1]

[1]*Division of Immunology, Department of Microbiology and Immunology, Institute of Medical Science, University of Tokyo,* [2]*Department of Pediatric Surgery, Nihon University School of Medicine, Tokyo, and* [3]*First Department of Internal Medicine, Kyorin University School of Medicine, Tokyo, Japan*

doi:10.1111/j.1365-2567.2005.02262.x
Received 22 July 2005; revised 22 August 2005; accepted 26 August 2005.
Correspondence: Dr Kiyoshi Takatsu, Division of Immunology, Department of Microbiology and Immunology, Institute of Medical Science, University of Tokyo, 4-6-1 Shirokanedai, Minato-Ku, Tokyo 108–8639, Japan. Email: takatsuk@ims.u-tokyo.ac.jp
Senior author: Takeshi Kikuchi, email: kikuchiT@ims.u-tokyo.ac.jp

Summary

The effector CD8$^+$ T cells recognize major histocompatibility complex (MHC) class I binding altered self-peptides expressed in tumour cells. Although the requirement for CD4$^+$ T helper type 1 (Th1) cells in regulating CD8$^+$ T cells has been documented, their target epitopes and functional impact in antitumour responses remain unclear. We examined whether a potent immunogenic peptide of *Mycobacterium tuberculosis* eliciting Th1 immunity contributes to the generation of CD8$^+$ T cells and to protective antitumour immune responses to unrelated tumour-specific antigens. Peptide-25, a major Th epitope of Ag85B from *M. tuberculosis* preferentially induced CD4$^+$ Th1 cells in C57BL/6 mice and had an augmenting effect on Th1 generation for coimmunized unrelated antigenic peptides. Coimmunization of mice with Peptide-25 and ovalbumin (OVA) or Peptide-25 and B16 melanoma peptide [tyrosinase-related protein-2 (TRP-2)] for MHC class I led to a profound increase in CD8$^+$ T cells specific for OVA and TRP-2 peptides, respectively. This heightened response depended on Peptide-25-specific CD4$^+$ T cells and interferon-γ-producing T cells. In tumour protection assays, immunization with Peptide-25 and OVA resulted in the enhancement of CD8$^+$ cytotoxic cell generation specific for OVA and the growth inhibition of EL-4 thymoma expressing OVA peptide leading to the tumour rejection. These phenomena were not achieved by immunization with OVA alone. Peptide-25-reactive Th1 cells counteractivated dendritic cells in the presence of Peptide-25 leading them to activate and present OVA peptide to CD8$^+$ cytotoxic T cells.

Keywords: antigen presentation; cytotoxic T cells; peptide; T helper 1 cells; tumour immunity

Introduction

The identification of tumour antigens has renewed interest in immunotherapy for cancer. There is a body of evidence that tumour-specific T cells recognize tumour-associated antigens on the cancer cells and play an essential role in inhibiting tumour growth and eradicating cancer cells.[1–3] CD8$^+$ cytotoxic T lymphocytes (CTL) from specifically immunized mice are capable of destroying tumour target cells *in vitro*[4] and adoptive transfer of CD8$^+$ T cells from immunized donors confers resistance to tumour transplants on naive mice.[5–7] As CD8$^+$ CTL can lyse tumour cells directly and destroy large tumour masses *in vivo*, much attention has focused on the role of CD8$^+$ T cells in the immunotherapy of cancer. Over the past two decades, a wide range of peptides derived from tumour cells of mice and humans that bind major histocompatibility complex (MHC) class I and are recognized by CD8$^+$ T cells has been defined.[1,8,9] However, in both clinical and animal studies, therapeutic strategies focused on the use of CD8$^+$ T cells and MHC class I-restricted tumour antigens have not been effective in eliminating cancer cells.

There has been a recent reappraisal of the role and importance of CD4$^+$ T helper (Th) cells in antitumour responses, because CD4$^+$ Th cells are required for generating and maintaining potent antitumour immunity.[5,6,10] The role of CD8$^+$ and CD4$^+$ T cells in tumour systems has been the object of intense interest. A major obstacle for the development of optimal cancer vaccines is the lack of effective methods for identifying MHC class

II-restricted tumour antigens that can stimulate $CD4^+$ T cells.[11,12] Identification of such antigens would provide new opportunities for developing effective $CD8^+$ CTL and would improve our understanding of the mechanisms by which $CD4^+$ T cells regulate the host immune system.

A variety of tumour-derived antigens have been defined by immunoglobulin G (IgG) antibodies in sera taken from tumour bearers with serological identification of antigens by recombinant expression cloning (SEREX).[13–16] The SEREX repertoire can be considered a reflection of the $CD4^+$ T-cell repertoire. Shiku and his colleagues reported that coimmunization of mice with plasmids encoding these SEREX-defined wild-type antigens and mutated mitogen-activated protein kinase 2 (mERK2; containing tumour-specific CTL epitope 9m of CMS5) led to a profound increase in $CD8^+$ T cells specific for mERK2.[13] This heightened response depends on $CD4^+$ T cells and on the copresentation of SEREX-defined wild-type antigens and the CTL epitope. Their results indicate the essential role of $CD4^+$ T cells in mediating the increased $CD8^+$ T-cell response and tumour inhibition induced by coimmunization with SEREX-defined antigens.

We have reported that immunization of *Mycobacterium tuberculosis*-primed mice with purified protein derivative (PPD)-modified attenuated X5563 myeloma cells induces an X5563-specific $CD8^+$ CTL response and antitumour immunity.[17–19] We infer from these results that *M. tuberculosis*-derived proteins or peptides may enhance the $CD8^+$ CTL response and antitumour immunity by coimmunization with tumour antigen or neo-tumour antigen. Ag85B, one of the major proteins secreted by *M. tuberculosis*, elicits a strong Th1 response *in vitro* in T cells from both PPD-positive asymptomatic human subjects and Ag85B-primed cells of C57BL/6 ($I\text{-}A^b$) mice. Peptide-25 (amino acids 240–254) of Ag85B, which is the most potent antigen species yet purified for both humans and mice, is a major Th1 cell epitope of Ag85B. Active immunization of C57BL/6 mice with Peptide-25 induces the differentiation of $CD4^+$ T-cell receptor (TCR) $V\beta11^+$ T cells that produce interferon-γ (IFN-γ) and tumour necrosis factor-α (TNF-α)[20–23].

We investigated whether Th1-inducible Peptide-25 intensifies the $CD8^+$ CTL response to unrelated tumour-specific antigens through stimulation of a $CD4^+$ Th1 cell response leading to the induction of antitumour immunity that is effective in eliminating cancer cells. We also discuss the possible mechanisms of Peptide-25-induced enhancement of the $CD8^+$ CTL response.

Materials and methods

Mice

C57BL/6 mice were purchased from Charles River Japan (Tokyo, Japan). Peptide-25-reactive TCR transgenic (Tg) (P25 TCR-Tg) mice were generated and maintained as described previously.[24] IFN-γ deficient ($IFN\text{-}\gamma^{-/-}$) mice[25] were kindly provided by Dr Y. Iwakura (Institute of Medical Science, University of Tokyo, Tokyo, Japan). Ovalbumin (OVA)-specific TCR-Tg (OT-1) mice were kindly provided by Dr T. Hirano (Osaka University, Suita, Japan). These mice were housed in the animal facility at the Institute of Medical Science, University of Tokyo, under specific pathogen-free conditions, and were used at 8–12 weeks of age.

Antigens and reagents

Peptide-25 (FQDAYNAAGGHNAVF), Peptide-9 (DWY SPACGKAGCQTY), and Peptide-18 (AGGYKAADM WGPSSD) of Ag85B were synthesized by Funakoshi Co., Ltd (Tokyo, Japan). Purified chicken OVA was purchased from Sigma-Aldrich, Co. (St Louis, MO). MHC class I-binding OVA Peptide (SIINFEKL) and B16 melanoma peptide tyrosinase-related protein-2 (TRP-2) (VYDF FVWL)[26] were also synthesized by Funakoshi Co., Ltd.

Culture medium

RPMI-1640 (Gibco BRL, Grand Island, NY) supplemented with 10% (v/v) heat-inactivated fetal calf serum (Sigma-Aldrich, Co.), 50 μM 2-mercaptoethanol, 100 IU/ml penicillin G and 50 μg/ml streptomycin was used as the complete medium for cultures throughout the present experiment.

Cell lines

The murine thymoma line, EL-4 ($H\text{-}2K^b$) was purchased from the American Type Culture Collection (Rockville, MD). EL-4 transfectant of the OVA gene (E.G7 cells) was kindly provided by Dr H. Udono (Nagasaki University School of Medicine, Nagasaki, Japan) and the B16 melanoma cell line was kindly provided by Dr H. Tahara (Institute of Medical Science, University of Tokyo, Tokyo, Japan).

Immunization

Mice were immunized by subcutaneous injection on the abdomen with OVA (10 μg/mouse) emulsified in incomplete Freund's adjuvant (IFA), Peptide-25, or its related peptide (10 μg/mouse) in IFA or a mixture of OVA (10 μg/mouse) and Peptide-25 (10 μg/mouse) in IFA as described previously.[21] In some experiments, mice were immunized with OVA (10 μg/mouse) in IFA on the left-hand side of the abdomen and with Peptide-25 (10 μg/mouse) in IFA on the right-hand side of the abdomen. We also immunized mice with MHC class I-binding TRP-2 peptide (10 μg/mouse) in place of OVA.

In vivo *and* in vitro *T-cell depletion*

$CD4^+$ T cells were depleted *in vivo* by the administration of 0·3 mg monoclonal antibodies (mAbs) against CD4 (GK1.5) on days −13, −12, −11, −6, −5, −4, +1, +2 and +3 relative to immunization. Fluorescence-activated cell sorter (FACS) analysis of blood mononuclear cells from GK1.5-treated mice at the time of immunization confirmed the effectiveness of the $CD4^+$ T-cell depletion. *In vitro* T-cell depletion was achieved by the incubation of spleen cells with either the IgM subclass of mAb against CD4 or CD8 and guinea-pig complement. FACS analysis of the treated spleen cells confirmed the effectiveness of the depletion.

In vitro *CTL induction and $CD8^+$ cytotoxic T-cell assay*

In vitro CTL induction and $CD8^+$ CTL assay were carried out according to previously described methods[17,18] with slight modification. Ten days after immunization with OVA in IFA or OVA and Peptide-25 in IFA, spleen cells (1×10^7) were cultured *in vitro* with γ-irradiated (20 000 rad) E.G7 cells (8×10^5). Spleen cells from TRP-2-immunized mice were stimulated *in vitro* with TRP-2 (10 μg/ml). After 5 days in culture, the CTL activity of the resulting effector cells was assayed. Target cells (E.G7, EL-4, and B16 melanoma cells) were labelled with ^{51}Cr (Perkin Elmer Life Science, Boston, MA) at 37° for 40 min. After washing, ^{51}Cr-labelled target cells (1×10^4) were incubated with effector cells at various effector cell to target cell ratios. Release of ^{51}Cr was measured in the supernatants that were harvested after 4 hr incubation. Maximum release was measured by resuspending the target cells in lysis buffer containing 0·1% Triton-X-100. Spontaneous release was obtained from target cells incubated with medium alone and was less than 10% of maximum ^{51}Cr release. The percentage specific lysis was calculated according to the following formula, where c.p.m. represents counts per minute: percentage specific lysis = $[(\text{c.p.m.}_{\text{experimental release}} - \text{c.p.m.}_{\text{spontaneous release}})/(\text{c.p.m.}_{\text{maximum release}} - \text{c.p.m.}_{\text{spontaneous release}})] \times 100$.

A dose–response curve of effector cells was established in all experiments and the number of lytic units (LU) was calculated as previously described.[19] In these calculations 1 LU was arbitrarily defined as the number of spleen cells required to achieve 50% lysis of 1×10^4 ^{51}Cr-labelled target cells during a 4-hr incubation.

Tumour challenge experiments

Three groups of 12 mice were immunized by subcutaneous injection of the abdomen with OVA (10 μg/mouse) in IFA, Peptide-25 (10 μg/mouse) in IFA, or a mixture of OVA (10 μg/mouse) and Peptide-25 (10 μg/mouse) in IFA. Twelve mice were injected with IFA without any protein or peptide to act as a control group. Ten days after the immunization, all mice were challenged by subcutaneous injection with E.G7 (5×10^5 cells/mouse) on their backs. In some experiments, B16 melanoma cells (5×10^5 cells/mouse) were transplanted in TRP-2-immunized mice. Tumour size was assessed using a microcaliper a 2-day to 3-day intervals and was expressed as the square of the smallest diameter of the tumour multiplied by its largest diameter. The survival of the mice was also monitored periodically.

Frequency analysis of OVA-specific CTL

The frequency of OVA-specific CTL in spleen cells after immunization was measured using OVA peptide-loaded H-$2K^b$:Ig protein (BD Biosciences Pharmingen, San Diego, CA) according to the manufacturer's instructions. Spleen cells prepared from mice 10 days after immunization, were stained with 4 μg OVA peptide-loaded H-$2K^b$:Ig protein and incubated for 60 min at 4°. After washing, cells were stained with anti-mouse IgG1 (A85-1)–phycoerythrin (PE; BD Biosciences Pharmingen) and anti-CD8 (53-6.7)–fluorescein isothiocyanate (FITC; BD Biosciences Pharmingen) and incubated for 30 min at 4°. After washing, cells were analysed using FACSCalibur (Becton Dickinson, Mountain View, CA).

Assay for dendritic cell activation

Immature dendritic cells (DCs) were propagated *in vitro* by culturing $CD11c^+$ bone marrow cells with granulocyte–macrophage colony-stimulating factor (GM-CSF) (20 ng/ml) and interleukin-3 (IL-3) (20 ng/ml) for 6 days. To assess the expression of surface molecules and IL-12 production of DCs after Peptide-25 treatment, the cells obtained (5×10^5) were cocultured with Peptide-25 (10 μg/ml) in the presence of $CD4^+$ T cells (5×10^5) from P25 TCR-Tg mice for 48 hr. The expression of surface molecules on DCs was analysed by FACS. The IL-12 production was assessed by enzyme-linked immunosorbent assay (ELISA). To assess the antigen-presenting activity of DCs after Peptide-25 treatment, the cells obtained (5×10^5) were cocultured with $CD4^+$ T cells (5×10^5) from P25 TCR-Tg mice and 5-carboxyfluorescein diacetate succinimidyl ester (CFSE)-labelled $CD8^+$ T cells (5×10^5) from OT-1 mice for 96 hr in the presence of Peptide-25 (10 μg/ml) and OVA (10 μg/ml). After the culture, cell division cycles were determined by FACS analysis.[27]

Assay for cytokine production by intracellular cytokine staining and ELISA

For assessment of cytokine production of spleen cells from OVA- or TRP-2-immunized mice, spleen cells